Monitoring anthropogenic particles in the environment: recent 1 developments and remaining challenges at the forefront of analytical 2 methods 3 4 5 6 Karin Mattsson¹, Vitor Hugo da Silva², Amrika Deonarine³, Stacey Louie⁴, Andreas 7 Gondikas^{5,*} 8 9 **Affiliations** 10 ¹Department of Marine Sciences, Kristineberg Marine Research Station, University of 11 12 Gothenburg, Fiskebäckskil, Sweden ²Department of Bioscience, Aarhus University, Roskilde, Denmark 13 14 ³Department of Civil, Environmental and Construction Engineering, Texas Tech University, 15 Lubbock TX USA ⁴University of Houston, Houston, Texas, United States 16 ⁵Department of Geology and Geoenvironment, University of Athens, Athens, Greece 17 18 *Corresponding author (agondikas@uoa.gr National and Kapodistrian University of Athens, 19 Faculty of Geology and Geoenvironment, Panepistimioupoli Zografou, Athens, Greece, 20 21 15784) 22 23 **Keywords**; analytical techniques, microplastic, microparticle, nanoplastic, nanoparticle, 24 environmental monitoring 25 26 **Abbreviations** 3D – 3 dimensional AF4 – asymmetric flow field flow fractionation AFM – atomic-force microscopy BSE - back scattered electron CCD – charged couple device CFFF – centrifugal or sedimentation field flow fractionation CryoTEM – cryogenic transmission electron microcopy DLS - dynamic light scattering DLSI – dispersive light scattering image EDS/EDX – energy dispersive x-ray spectroscopy ENM - engineered nanomaterials FAST – fast acquisition speed technique FFF - field flow fractionation FOQELS – fiber optic quasi-elastic light scattering FPA – focal plane array FTIR - fourier transformed infrared HF-FFF - hallow fiber field flow fractionation m-PTA – multispectral particle tracking analysis MALS – multi-angle or static light scattering MApNTA – maximum a posterior nanoparticles tracking analysis

NIST – National Institute of Standards and Technology

NP - nanoparticles

NTA – nanoparticle tracking analysis

PE - polyethylene

ppb – part per billion

PS – polystyrene

PTA – particle tracking analysis

Py-GCMS – pyrolysis gas chromatography mass spectroscopy

QCL - quantum cascade laser systems

S-SNOM - scattering-type near-field optical microscope

SE – secondary electrons

SEM – scanning electron microscopy

SERS – surface enhanced Raman scattering

siMPLE – systematic identification of microplastic in the environment

SNOM – scanning near-field optical microscope

SP-DLS – single particle dynamic light scattering

spICPMS single particles inductively coupled mass spectroscopy

SRS – stimulated Raman scattering microscopy

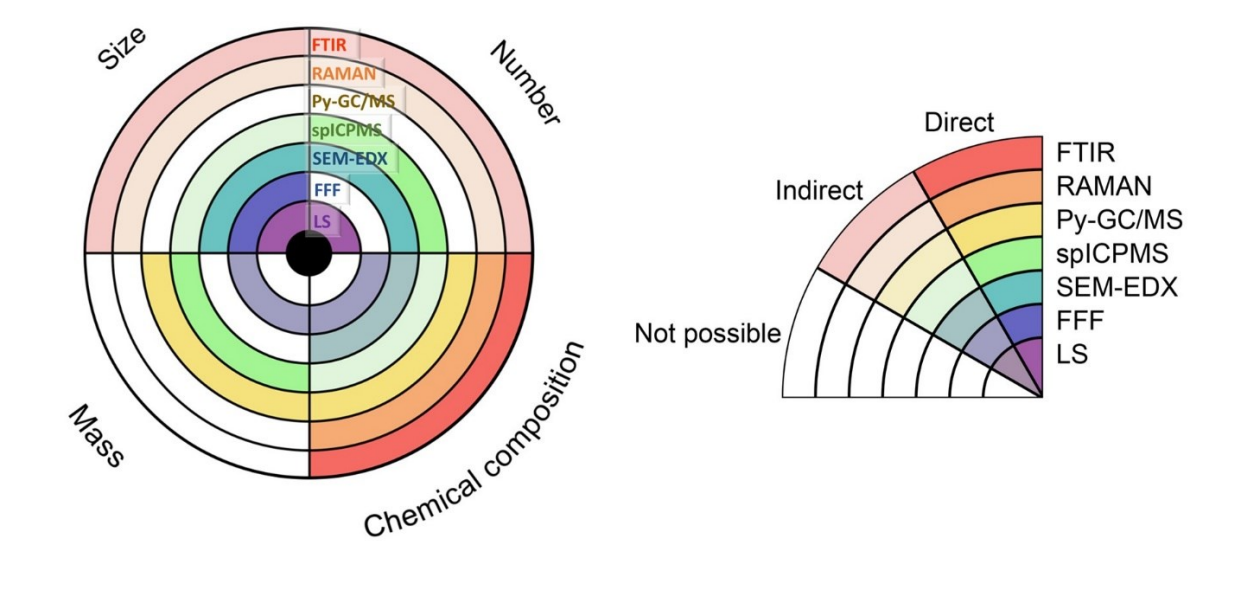
STEM – scanning transmission electron microscopy

TEM – transmission electron microscopy

TRWP – tyre and road wear particles

UV-vis – ultraviolet visible

Graphical abstract



Abstract

 Anthropogenic particles at the micro- and nano-scale are posing risks to human health and the ecosystem. Engineered nanomaterials, micro- and nano-plastics, soot, road and tire wear are a few prominent examples of particles that are either intentionally manufactured or incidentaly produced and released into the environment. Analytical developments in the past few decades have made possible to study particles in the micro- and nanoscale, however there is still no universal protocol of analysis and caveats exist in the use of the most prominent techniques. The task is challenging due to the large variety of particle properties and the complexity of environmental media. This review discusses a selected group of techniques most likely to play a key role in future monitoring activities and discuss recent developments and inherent shortcomings.

49 1. Introduction

Anthropogenic particles are a broad category of particles manufactured (engineered) or incidentally produced by human activities. These particles can be released either intentionally or unintentionally into the environment, potentially causing adverse health effects and ecosystem impairment. This category of particles includes engineered nanoparticles, plastic particles (micro and nano), soot, paint flakes, tire and road wear particles (TRWP), as well as other combustion and friction particulate byproducts. Many of them are known to cause health effects and/or contain toxic compounds.

Anthropogenic particles (organic and inorganic) can be found in a wide range of sizes and those on the micro and nano scales are currently receiving attention from society and governments around the world due to the increased awareness of their existence and potential harmful consequences. Microlitter generally refers to particles debris ranging from 1 µm up to 5 mm in length, whereas environmental nanoplastic is defined as plastic particles between 1 nm and 1000 nm [1]. However, engineered nanomaterials are typically defined as solids with at least one dimension smaller than 100 nm, while it has been proposed that a threshold of 30 nm ought to be used instead, since novel functionalities become prevalent at this size range [2]. Here, the term "nanoparticles" is used to describe anthropogenic particles with size < 1 µm, including both nanoplastic and engineered nanomaterials. Regardless of size categorization, both anthropogenic micro- and nanoparticles have been detected in several environmental compartments, such as air [3], freshwater and marine water bodies [4,5], soils [6], marine sediments [7], aquatic organisms [8], as well as food and food packaging [9,10] and in the human body [11]. Overall, the number of particles found in the environment increases exponentially as particle size decreases [12] and it is the smaller size fractions that are more likely to induce adverse effects, owing to their reactivity, ability to pass through biological membranes (e.g. organ tissue) [13], transport behavior, and potential to be mistaken for food by organisms. Towards the smaller particle size, the particle analysis is arguably more complex with several analytical challenges ranging from sampling to particles characterization.

Since anthropogenic particles vary greatly in terms of composition, size and morphology, there is no single analytical method that covers these features entirely, and different analytical techniques are applied to assess these pollutants in the environment. The scientific community has been developing analytical methods aiming mainly at specific categories of particles and applying different analytical techniques to address the multiple scientific questions regarding the anthropogenic particles and their effects. In general, these methods apply frontier techniques to overcome several challenges posed by the particle's features, mainly size limitation. To address the multiple scientific questions related to the occurrence, environmental fate and toxicity of anthropogenic particles, there have been advancements in analytical methods and techniques, particularly with respect to throughput analysis and lower limits of detection for particle size and mass or number concentration.

This paper provides a review of the most used analytical techniques for separation, characterization, and quantitation of anthropogenic micro- and nanoparticles. These techniques fulfill one or more of the following criteria and are considered fitting for a broad range of applications: (i) parameters measured are relevant to characterize and/or determine particle abundance (number of particles, size distribution, composition, total mass and mass per particle); (ii) versatility in application to environmental compartments and particle characteristics (e.g. organic or inorganic); (iii) limits of detection that are relevant for environmental studies. (iv) technology maturity and instrument availability; (v) ease of use and established algorithms for data interpretation. The techniques included in this review are

Fourier-transformed infrared Raman spectroscopy, spectroscopy, pyrolysis chromatography mass spectrometry, single particle inductively coupled mass spectrometry, electron microscopy, and field flow fractionation with light scattering. In the following sections, an overview of each technique is presented, followed by a discussion of specific analytical challenges and limitations, recent advances (~5 years), and new directions. We address the qualitative and quantitative aspects of each technique along with challenges related to sample preparation and treatment, interferences and artefacts, and data analysis and interpretation. It is intended that this review serve as a basis for addressing challenges in producing quality data for monitoring activities and investigations on the abundance, fate, and toxicity of anthropogenic particles, which are urgently needed in risk assessment and regulatory efforts.

2. Vibrational spectroscopy

2.1 Fourier-transformed infrared spectroscopy

Fourier-transformed infrared (FTIR) spectroscopy is one of the most common techniques used for the characterization of microplastics in the environment. This technique measures the transition of molecular vibration states by the absorption of infrared radiation, in which the photon energy is transferred to the molecules, changing their vibrational state. For a molecule to absorb infrared radiation there must be a variation in the dipole moment due to its vibrational or rotational movements, such as the polymeric materials [14]. As a result, characteristic spectra profiles of the analyzed material are obtained with fast and nondestructive measurements, requiring little or no sample preparation [15,16]. Infrared instruments can be combined with optical microscopes (µ-FTIR) for hyperspectral image acquisition, simultaneously collecting chemical and spatial information of several particles at the same time by automated sample mapping [14]. Hyperspectral images bring several advantages for microplastic analysis, where a sample after purification can be filtered directly on a membrane (transparent at infrared range) for mapping, allowing the characterization and quantification of microplastic particles and the evaluation of their morphological features (size distribution, area, etc.) without manual sorting.

Similarly to conventional infrared instruments, infrared microscopes are flexible and different measurement modes (Figure 1) can be applied for spectra acquisition, e.g. transmittance, reflectance and attenuated total reflectance (μ -ATR) [16]. Each measurement mode should be applied according to the particles' features and size, as summarized in Table 1. ATR measurements provide the best spatial resolution and the reflective crystal must be in full contact with the particle to produce desirable spectra [17]. Therefore, particles smaller than the reflective crystal should be avoided in μ -ATR mode. Transmittance is well suited for sample mapping and it is the most common approach used for microplastic analysis. In this mode, the source light is transmitted through the sample and particles thicker than 300 μ m provide weak or no analytical signal due to total light absorption [16]. On the other hand, this limitation can be overcome when reflectance mode is used. However, this measurement mode depends on the particle morphology; there can be light reflection errors due to the light scattering and samples with a wide range of particle sizes can face challenges in defining the camera focus for quality spectra measurements [15].

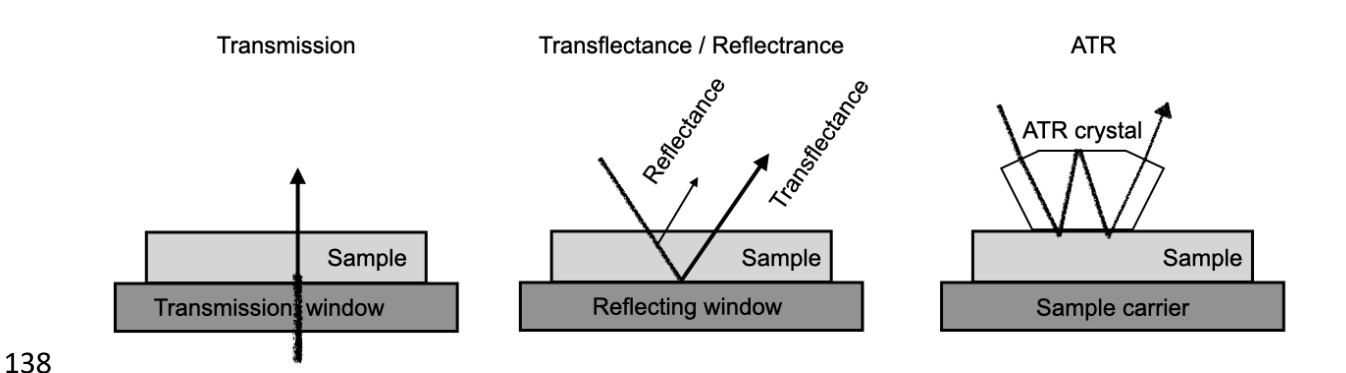


Figure 1. Overview of the measurement modes applied to μ -infrared spectroscopy. Figure adapted from Ref. [16].

Hyperspectral image measurements can be time consuming, mostly depending on the detector applied in the instrument, such as single point or focal plane array (FPA). Unlike single-element detectors, FPA-based imaging uses several detectors placed in a grid pattern for area mapping, improving the measurement time and analysis throughput [18]. Even faster analysis can be obtained with recently developed Quantum Cascade Laser systems (QCL), where an FPA-based instrument is combined with high brilliance infrared sources based on broadly tunable external cavity quantum cascade lasers. Although this system also analyzes larger areas with 14 times more pixels than a high-end μ -FTIR instrument, measurements are often limited to the fingerprint region, in which important peaks for polymer identification are missing, such as the CH and OH signals in the range from 3600 to 2750 cm⁻¹ [19].

Most of the μ-FTIR instruments can reach small pixel sizes (~1 μm) and detailed information about small particles can be obtained. However, it should be noted that the smallest detectable particle size in infrared microscopy is determined by the microscope diffraction limit (e.g. 10 μm at 1000 cm⁻¹), regardless of the pixels size applied [17]. For infrared analysis of particles below the diffraction limit, more advanced techniques must be applied such as nano-FTIR, which is a combination of a scattering-type near-field optical microscope (s-SNOM) with a broadband infrared source [20,21]. This technique is based on atomic-force microscopy (AFM), where a probe tip is approached to the sample, creating a nano-focus for surface measurement with a spatial resolution that depends on the radius of the cantilever tip, which is up to 20 nm [22]. Nano-FTIR has been demonstrated for nanoplastic analysis, and further advancement and investigation of this developing technology needs to be explored [20].

Infrared microscopy has been successfully applied for microplastic analysis with several publications worldwide applying this technique for analysis of this anthropogenic litter in sediment [23–25], water [26,27] and biota [9,28] samples. Although the feasibility of this technique has been demonstrated, the analysis protocol needs to be harmonized for more accurate data comparability, such as the filters applied to reduce interferences and sample pretreatment to avoid organic matter and biofilm that can hide the polymer signal.

2.2. Raman Spectroscopy

Raman spectroscopy is a technique based on the inelastic scattering from monochromatic light, such as laser light. As light interacts with the sample, photons are absorbed and re-emitted with a shifted frequency. The shift provides information about vibrational, rotational, and low-frequency transitions in molecules, resulting from changes in their dipole moment while absorbing radiation. Micro-Raman spectroscopy is the combination of Raman spectroscopy with optical microscopes, making it possible to focus the excitation light on a small spot [17]. However, nowadays, most Raman microscopes are confocal, which gives a weaker Raman signal but provides a higher depth resolution and image contrast. Raman is a single particle method, which simultaneously provides chemical information of each measured particle, as well as its size and morphology. The analysis can be done in two ways, imaging, or particle measurement. For imaging measurements, the entire substrate or a section is scanned, and a spectrum is received from each image pixel. For particle measurements, the analysis is done in two steps, first an optical image is acquired with a light microscope and then the spectra are acquired where particles are detected. Both methods are three-dimensional with two spatial dimensions and one spectral dimension.

The main advantage of Raman microscopy is the detection limit, around 1 µm, in addition to not being sensitive to water signal as infrared spectroscopy [19]. A limitation with Raman spectroscopy is the weak signal it provides, where less than one in a million excitation photons give rise to a single Raman photon [29]. This problem can be overcome applying longer integration time. However, longer exposure can degrade the sample, and this should be done carefully. Raman spectra may have problems with cosmic ray events generated when high-energy particles pass through the detector and generate many electrons that the detector interprets as a signal. However, by recording more than one spectrum, the problem will be neglected. Additionally, Raman spectra can suffer from a fluorescence background, which can be more than six orders of magnitude higher than the efficiency of the Raman interactions. To reduce the fluorescence signal, it is possible to change the excitation wavelength or reduce the detection volume. There is less fluorescence using a confocal Raman since it only collects photons emitted from the focal plane [30]. Impurities and organic matter can also cause fluorescence and can be reduced by cleaning the particles before the analysis. The cleaning procedure might degrade the plastics and must be done carefully.

The intensity of the Raman scattering is proportional to v^4 , where v is the frequency of the laser. Shorter wavelengths lead to higher Raman signals, but many samples show strong fluorescence when excited with shorter wavelengths such as 400 nm [30]. Shorter excitation wavelengths give higher lateral resolution $(0.61 * \lambda/NA)$, where λ is the laser wavelength, and NA is the numerical aperture, showing that both factors are equally important. The Raman signal is proportional to excitation power; however, the excitation power can cause thermal decomposition because of absorption. Other common problems with Raman spectroscopy are interfering signals from the underlying substrate, additives, fillers, dyes, or coloring agents that can affect the spectra (Figure 2).

Recently, Raman microscopy has been used to identify microplastic particles in environmental samples such as in wastewater, seawater [31], sediment [32,33], mineral water [34], drinking water [35] and air [3]. In general, two workflows have been used: (i) visual identification where a subset of suspected microplastic particles has been moved and identified with Raman and (ii) direct particle identification on filters of different substrates such as polycarbonate or silicon filter [31]. The first workflow is not optimal since smaller particles are hard to visually identify and it is not possible to move them with tweezers. It also relies on visual identification and there can be many false negatives, i.e., particles that are not visually identified as plastics but are

plastics. The second workflow works for smaller particles and it is possible to identify all particles, however, often only a subset of the filters is analyzed to reduce running time.

Raman spectroscopy can also be used for analysis of single molecules on solid surfaces by applying surface-enhanced Raman scattering (SERS). Molecules are adsorbed onto a metal surface, which enhances their Raman scattering by factors of up to 10^8 [36]. SERS has therefore been applied to detect metallic nanoparticles, however challenges pertaining to high variability, interferences from sample matrix and impurities, and the presence of "SERS hotspots" dominating the signal [37]. A few studies have used SERS to identify plastic particles in the nanometer size range in environment matrices such as seawater [38] and river water [39], as well as atmospheric particles [40]. Another Raman approach is stimulated Raman scattering microscopy (SRS), which is a technique where two laser beams are used, one that has a higher photon energy and one with a lower photon energy. It is faster than confocal Raman microscopy since it only measures signals at single wavenumber and it is less sensitive for fluorescence. However, since it only measures one wavelength, identification of different polymers is difficult. For instance, Zada *et al.* [41] used six wavenumbers to be able to identify five polymer types.

Confocal Raman microscopy has been gained more information about the samples such as Raman-AFM [42], Raman-SNOM [43] and Raman-SEM [44]. Raman tweezers, a combination of optical tweezers with Raman spectroscopy, has been used to identify micro- and nanoplastics in solution [45], and can further be combined with field flow fractionation (FFF) to identify size-fractionated polymers and inorganic particles between 200 nm and 5 μ m in diameter [46]. Nevertheless, Raman imaging has been used to identify plastic particles down to 100 nm [47–49].

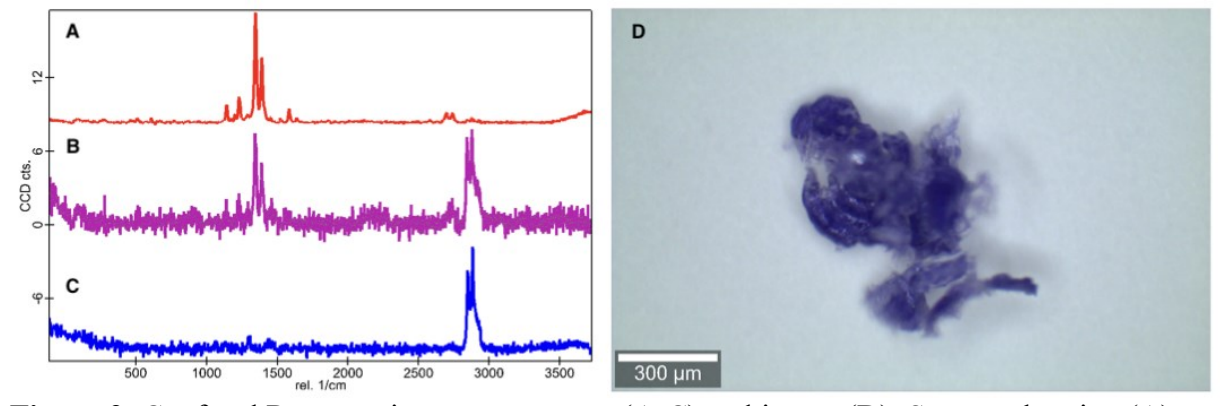


Figure 2: Confocal Raman microscopy spectra (A-C) and image (D). Spectra showing (A) mainly the dye, (B) both dye and polymer (C) only polymer.

2.3 Raman and FTIR data analysis

Raman and FTIR are complementary vibrational spectroscopies that have great similarity in the way their data are processed. In general, the data set for both techniques is complex and quite large when hyperspectral images are obtained. For microplastic analysis, where these techniques are massively applied, the most common data processing pipeline is the use of library search and multivariate data analysis for particle characterization based on the spectra information. Library search is currently the most common strategy applied for both Raman and

μ-FTIR. This approach compares the sample spectra with a reference library for matching and assigns the spectra when the similarity surpasses a given threshold [18,24,50]. Pearson's Correlation or Euclidian distance commonly determines the spectral similarity and the results often only rely on this index, which is a potential source of error due to its dependence on the spectral library and the threshold applied. Despite the fact that the spectral match depends heavily on the reference library comprehensiveness, this straightforward approach does not require an expert operator to acquire the information [15]. This analysis may last from a few seconds to several hours and depends on the size of the data set, since all the spectra must be compared with all the reference spectra in the matching routine. These reference spectra libraries can be purchased or customized, with specific spectra libraries already published for microplastic analysis using Raman [51] and μ-FTIR spectroscopies [52], as well as dedicated software for this purpose, such as siMPLe software [53].

Alternatively, multivariate data analysis (chemometrics) is well suited to retrieve the microplastic information for these complex data, with their feasibility already demonstrated by several publications in the literature. The typical multivariate analysis procedure consists of: (1) data processing to eliminate spectral interferences [16]; (2) exploratory analysis to identify patterns in the dataset [54] and; (3) modeling to develop statistic models to retrieve the plastic information based in the representative sample spectra [15,55–57]. Chemometric approaches are validated, and a statistical evaluation of the models are performed to reduce bias and increase confidence in the particles/spectra assignment. This analysis strategy is faster than the traditional library search with results obtained in a few minutes once the classification models are developed, and morphological information about the particles is possibly obtained. The use of chemometrics for image analysis is well established; however, it needs to be further explored for microplastic analysis, to better understand and extract as much information as possible from these complex data and provide more accurate results and robust statistical models for high throughput analysis.

3. Pyrolysis gas chromatography mass spectrometry

In pyrolysis - gas chromatography mass spectrometry (Py-GCMS), the samples are thermally decomposed in a pyrolysis step, followed by separation of the degradation products using gas chromatography, ionization, and further fragmentation, and finally detection of the ionized fragments using mass spectrometry (Figure 3). Py-GCMS is commonly used to identify and determine the mass concentrations of anthropogenic particles such as plastics and TRWP. Identification of the thermal degradation products provides structural and compositional information about the particles in the sample and allows the determination of mass concentrations of specific compounds per unit of mass or volume of the sample.

Multiple Py-GCMS approaches have been used in the analysis of plastic particles and TRWP.
These involve various thermal programs or configurations of the pyrolysis step, such as singleshot Py-GC/MS (single temperature, > 500°C) [58–60], sequential Py-GCMS (variable
temperature, from low to high) [61], thermal desorption pyrolysis (concentration of degradation
products onto adsorbent media, followed by release through heating of adsorbent) [62] and
thermochemolytic Py-GCMS (allows chemical reaction to occur which makes the detection and
identification of degradation products easier) [63].

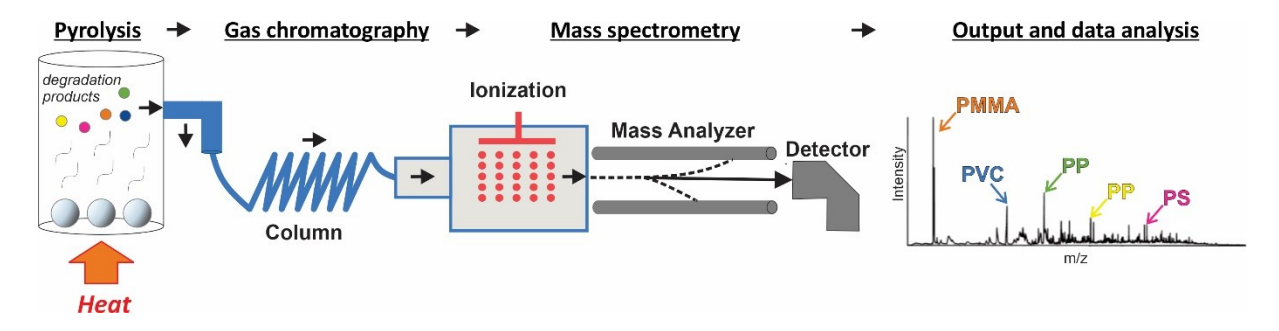


Figure 3. Schematic of pyrolysis-GCMS for analysis of plastic particles

Py-GCMS is a complementary technique to vibrational spectroscopies, which in addition to providing information on sample composition, delivers quantitative information on the mass of specific polymers, from which the polymer mass concentration per unit mass (e.g., per g sediment) or volume (e.g., per liter water) can be calculated. This is in contrast to FTIR and Raman, which can provide particle number concentration only. The ability to provide mass data is a strength of Py-GCMS. Mass data are critical for investigations of fate and transport as well as exposure and toxicity, such as in mass balance approaches for studying transformations and bioaccumulation and the development of reference doses which are given in units of g per kg body weight. In addition, Py-GCMS analyzes all particles at both nano- and micro-scale, providing a more accurate understanding of the particle composition and structural complexity, including differentiation between plastic polymers and organic additives. However, unlike vibrational spectroscopies, Py-GCMS is a destructive technique, and the sample cannot be reanalyzed in case of non-successful data collection.

Py-GCMS has successfully been used for the analysis of micro- and nanoplastics and TRWP in a variety of environmental and biological media, such as sediments, soils, air, surface runoff, suspended particulate matter, sewage sludge and aquatic organisms [60,64–66]. Py-GCMS has been used for the analysis of single and bulk plastic particles which first have been isolated from the sample media (e.g. [61]), as well as for the direct quantification of plastics without particle isolation, such as through the use of accelerated solvent extraction to extract polymers from the sample matrix (e.g. [67],). With respect to particle size and mass limits, polymer mass detection limits below 1 μg have been achieved, with the mass detection limit as a function of the polymer type [58]. The minimum size in which a single particle can be analyzed is limited by the feasibility of isolating and transferring it to the sampler system. The smallest single particle which has been analyzed using Py-GCMS had a diameter of 500 μm [68,69]. The smallest bulk particles which have been analyzed thus far are nanoplastic particles with diameter < 1 μm [70].

A major challenge in Py-GCMS is the identification of polymers in complex environmental and biological matrices. The matrix complexity can result in high background signals and interferences from natural organic matter (e.g., naturally occurring proteins, fats, polysaccharides) with structures similar to the polymer degradation products and their ionization fragments. Sample processing methods for the concentration of polymers and removal of potential matrix interferences and background signals have been employed to improve the signal to noise ratio and lower mass detection limits. This includes: sample digestion followed by polymer preconcentration [63], pressurized liquid extraction onto silica gel [60], and pre-cleaning steps to remove natural organic matter from the particle surface, for example, by means of methanol extraction, enzymatic and/or oxidative decomposition.

However, sample pre-treatment procedures that are too aggressive can result in alteration of the particle prior to analysis [63,71–75].

342

343 344

345

346

347 348

349

350

351

352 353

354 355

356 357

358

359 360

361 362

363

364

365 366

367

368

369 370

371

372373

374

375376

377

378

379

380

381

Additionally, methods for improved data analysis and interpretation of pyrograms which increase the certainty of polymer and/or additive identification are currently being explored, such as the development of optimized Py-GCMS methods for specific polymers/additives; the identification of common interferences from various sample matrices; principal components analysis to identify specific polymer indicators; selected/single ion monitoring to compensate for background effects; and methods of reducing artefact formation, such as the use of deuterated internal standards [76]. A comprehensive, freely accessible shared database for thermal degradation and ionization products and polymer indicator ions (e.g., Tsuge et al. (2011) [77], NIST and Wiley mass spectra libraries) would be tremendously helpful for Py-GCMS users. To date, only a limited number of plastic polymers and additives have been identified, suggesting that this technique needs to be further explored. Future development of this method can benefit from advances in miniaturization of mass spectrometers, with portable mass spectrometry becoming relatively common in air quality monitoring [78]. A custom portable Py-GCMS has recently been developed by Zhang et al. and holds promise for providing rapid, in-field identification and mass quantification of microplastics [79], e.g. for marine sampling and monitoring.

4. Single particle inductively coupled plasma mass spectroscopy

Single particle inductively coupled mass spectroscopy (spICPMS) has evolved as a premium method for quantifying particles in complex aquatic matrices and one of the very few methods that may provide both number concentration and size distribution of particles in suspension. ICPMS instruments are used for the quantification of the majority of elements in the periodic table of elements, based on the mass-to-charge ratio. Prior to its application in particle analysis, ICPMS has been used for decades in the determination of metals at trace concentrations in aciddissolved samples, due to its high sensitivity and elemental selectivity. Because of its wide use in trace metal analysis, the technology is well established and is readily available for spICPMS analysis, although some software and hardware upgrades may be necessary for some models. Briefly, the liquid sample is mixed with argon gas at the tip of a nebulizer to produce a spray of droplets. Larger droplets are removed in a spray chamber while finer droplets are directed to a plasma torch (6000 – 8000 Kelvin), where the sample is desolvated, vaporized, atomized, and ionized. The charged atoms are then separated under an electric field, based on their mass to charge ratio, and detected. When a particle enters the plasma torch, a plume of ionized atoms is generated, which is detected as a spike (particle event) over the background signal (Figure 4). The number of spikes detected is used to derive the number concentration of particles in the suspension, while the area under the particle event is used to derive the amount of analyte in single particles, which is then translated to particle size. Two critical conditions ought to be met: (i) the particle number concentration needs to be low enough to reduce the chance of more than one particles entering the plasma at the same time and (ii) the data reading frequency needs to be high enough to allow identification of the particle event over the background signal. For a detailed review of the method and its applications prior to 2016, the reader is directed to an exhaustive review by Montano et al. in 2016 [80].

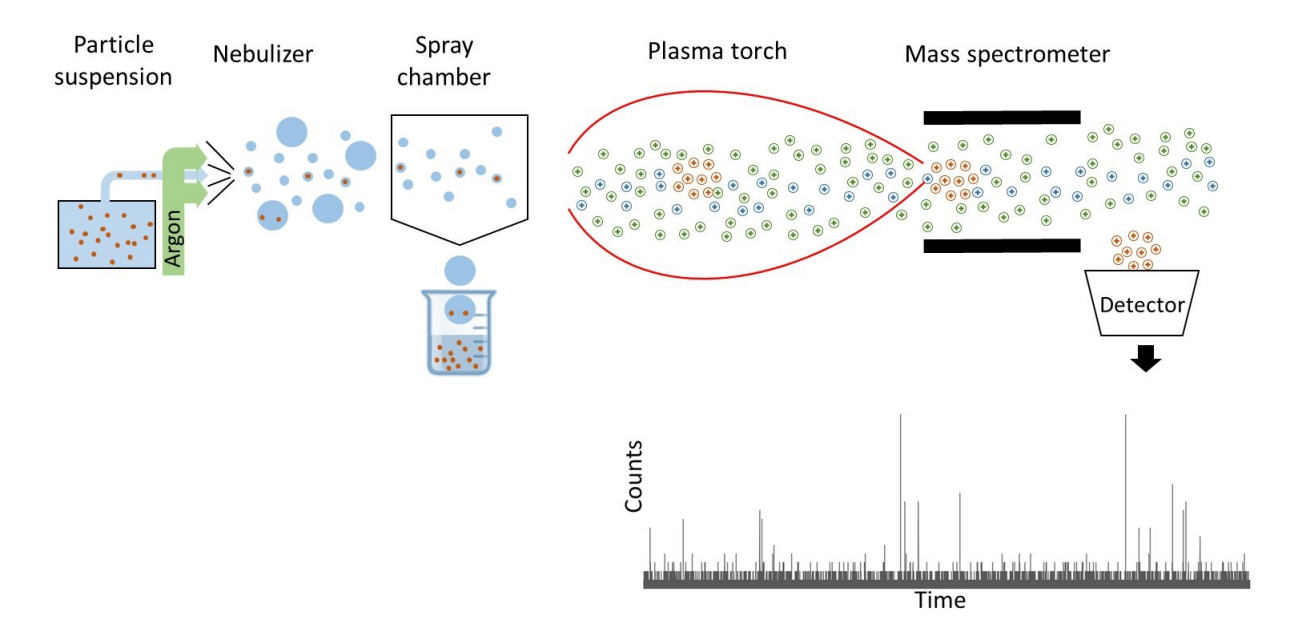


Figure 4. Schematic representation of particle analysis with spICPMS

 The technique has gained wide acceptance due to several key advantages: (i) high sensitivity that allows particles as small as 5 nm to be measured [81]; (ii) high selectivity, meaning that particles containing elements of interest are readily quantified; (iii) high through-put allows the analysis of a substantial number of samples within a reasonable timeframe and; (iv) readily available equipment, owing to the use of ICPMS for trace metal analysis. In addition, the parameters measured, i.e. particle number concentration and size distribution are key for the appropriate characterization of a particle suspension. However, keeping in mind that what is measured is the amount of one element during a particle event, the quantification of these parameters is challenged by analytical limitations and a complex data processing routine. An obvious challenge is the assumptions necessary to convert the analyte mass to size of a particle that is likely to contain other analytes, some of which may be impossible to measure with this technique (e.g. light elements such as oxygen and hydrogen). For this conversion, particle composition, density, and shape must be known. When these parameters have not been determined using complementary techniques, arbitrary assumptions are made, typically using the composition of the most common mineral of the target element, the density of the bulk mineral, and spherical shape.

Recent studies have improved the accuracy of particle size calculation from analyte mass, by improving the sample introduction system or using advanced instrumentation. Hyphenated methods are emerging as powerful tools with applications in complex matrices. Among them, asymmetric flow field flow fractionation (AF4) with its high-resolution size fractionation is used to force particles to enter the spICPMS in an orderly fashion, based on their size and shape. The method also removes dissolved components and concentrates particles of the same size, thus enabling the detectability of dilute samples with high dissolved background [82,83]. Hydrodynamic chromatography has also been applied for the determination of gold nanoparticles and their agglomeration state in gastrointestinal fluids [84] and the method has been validated for nanoscale liposomes [85]. Capillary electrophoresis also has been applied as a high through-put hyphenation technique with spICPMS for the detection of 10 nm gold nanoparticles [86]. Another approach to reduce uncertainties in size calculation is to utilize advanced instrumentation to quantify more than one element in single particles, thus acquiring

more complete information about their composition. A time-of-flight mass spectrometer enhanced with machine learning algorithms was used to distinguish naturally occurring from engineered cerium oxide nanoparticles, taking into account that natural particles are likely to contain other elements as "impurities" compared to their pristine engineered counterparts [87]. When hyphenated with AF4, a holistic set of data is acquired on the particle composition and structure and is probably the most advanced technique for the characterization of a nanoparticle suspension to date [88].

Another challenge for spICPMS is the detection of nanoparticles in samples with elevated background noise, which may be a result of dissolved components of the target analyte or interferences on the measured isotope. When the background noise is elevated, the intensity of spikes generated by small particles is challenging to distinguish from the fluctuating background signal, thus resulting in increased limits of detection. As already mentioned, hyphenation with AF4 will remove the dissolved background to a large extent. Due to the wide use of ICPMS in trace analysis, technical solutions developed to address polyatomic or isotopic interferences on the target analyte are also available for spICPMS. Sector field instruments utilize a magnetic field in addition to the electrostatic field, thus achieving high resolution between isotopes; in tandem ICPMS instruments, a collision and/or reaction gas mixture can be used to eliminate interferences [89,90]. A third approach to address the challenges imposed by elevated background is data treatment, where a threshold of 3 up to 7 times the standard deviation of the background is applied to separate background (below the threshold) and particle spikes (above). An improvement of the traditional threshold method is the deconvolution of the background from particle signals using a mixed Polyagaussian probability mass function [91]. Furthermore, by increasing the data acquisition frequency (FAST analysis), i.e. reducing the duration of signal acquisition window (dwell time), the background signal is reduced (by division in more dwell times) making particle events more prominent. Recently, a deconvolution method has been applied in combination with short dwell times to detect 20 to 100 nm silver nanoparticles in the presence of ppb levels of dissolved silver ions [92].

Until recently, spICPMS was not applied to measure carbon-rich particles, such as micro- and nano-plastics, due to the high ionization potential of carbon, which results in low ionization efficiency at the argon plasma. In addition, the background of 12C (the most abundant isotope of carbon) is very high in aqueous samples. However, when the 13C isotope is measured and the particle is large enough, carbon from particles can be detected above the background, as demonstrated for 1 – 5 µm spherical polystyrene microbeads dispersed in ultrapure water, i.e. without background from dissolved organic compounds [93,94]. Another approach for indirectly measuring plastic particles in the nanoscale has been demonstrated, using functionalized gold-containing nanoparticles, whose coating selectively adsorbs on carboxyl groups on the surface of nanoplastics; the metal from the conjugated nanoparticles is then detected with spICPMS [95].

In addition to the particle characteristics (composition, density, shape) and the background level, analysis with spICPMS is often hampered by the low concentration of nanoparticles in suspension and the multitude of organic and inorganic materials present, especially in environmental samples. To address this challenge, particle concentration and extraction techniques and novel sample introduction systems have been recently applied. A colloid extraction technique using surfactants [96] was able to extract all particles, irrespective of size or composition, and concentrate them in a smaller volume while maintaining particle integrity. A flow injection system was applied to dilute seawater samples, while minimizing the risk of altering particle stability [97]. Furthermore, enzymatic and chemical treatment has been applied

to decompose organic and inorganic material in complex matrices, thus simplifying the analytical task for spICPMS [98,99].

The spray chamber is a critical part of the sample introduction system and is used to protect the plasma torch from large droplets that would otherwise absorb heat and cause fluctuations in the plasma temperature, even causing the flame to extinguish. As a result of the droplet size discrimination, approximately 10% of the sample reaches the torch (the term transport efficiency is used to correct this effect), while the rest is discarded in the waste. Larger particles are less likely to survive the spray chamber, thus adding bias to the determination of the particle size distribution and number concentration. To address this issue, novel nebulization systems have been developed with direct injection of the sample, assisted by heating or gas displacement, achieving close to 100% transport efficiencies [100–104]. To accurately determine the transport efficiency, standard nanoparticle suspensions are necessary. However, these standards are not available for most elements, they are often not adequately characterized, and are prone to changes with time (losses on sample vials and pipette tips, gradual dissolution and/or aggregation, etc.). A microdroplet generator used to produce droplets of precisely defined size has been proposed to bypass the need for standard suspensions. Using solutions that contain pre-defined concentrations of dissolved components, it is possible to matrix-match a sample and conduct a calibration for the instrument response to the mass of analyte [105]. An alternative sample introduction system with application on solid samples is with laser ablation, with promising preliminary results on the achieved transport efficiency [106].

Overall, the analytical advantage of spICPMS is demonstrated by the wide range of its applicability in complex matrices, such as biological fluids [107], food [108], drinking water [109], surface waters [110], waste leachates [111], soil extracts [112], and plant extracts [113], among others. Identifying the most suitable components in terms of sample handling, sample introduction system, instrumentation, and data analysis algorithm depends on the target nanoparticles' physicochemical characteristics and the matrix [114]. It should be kept in mind, however, that the amount of analyte in each particle event may in fact originate from a particle comprised of various mineral forms (e.g. mix of iron oxides, crystalline and amorphous), a pure element (metallic silver or copper) or ions adsorbed on a larger particle (e.g. arsenic ions adsorbed on iron oxide particles). Distinguishing between these sources requires advanced instrumentation and possibly complementary techniques. Furthermore, data analysis is a complex process due to handling of large data files and the challenging separation of particles and background signals. Further hardware and software advancements are needed in these directions. Although the development of the micro-droplet generator offers an alternative, standard materials are a simple and cost-effective solution for calculating transport efficiency and calibrating the method, so further development in standard materials is also necessary.

5. Electron microscopy

463

464

465

466

467

468 469

470

471 472

473

474

475 476

477 478

479

480

481

482 483

484

485

486

487

488 489

490

491

492 493

494

495

496

497

498

499 500

501

502

503 504

505

506

507

Electron microscopy is a powerful tool for acquiring morphological information, such as size, shape, surface topography, and aggregate structure, in addition to qualitative and semi-quantitative elemental composition and crystal structure. The technique resembles the traditional light microscope instruments, but with substantially higher resolution, owing to the use of electrons instead of light. Similar to light microscopy, a sample is placed on a flat surface and areas of interest are magnified and examined. The electron beam is directed onto the sample and, through its interactions with the sample material, the particles morphology, composition, and crystal structure may be acquired. In transmission electron microscopy (TEM), a parallel electron beam is used, which penetrates the sample. High resolution morphological information can be obtained on particles up to 1 µm in thickness, while composition and crystal structure

may be obtained on particles up to 0.1 µm [115]. Although the accuracy and specificity of TEM are advantageous, the method is rarely used to characterize a population of particles in complex samples with an abundance of particles of diverse compositions and dimensions. The reason is that locating particles of interest is a time and effort consuming process, making it impossible to examine more than a few hundreds of particles per sample within a reasonable timeframe. Manually searching for particles of interest introduces operator bias, therefore TEM is often used as a complementary technique to verify the presence of target particles. In combination with bulk elemental analysis of filtered fractions, it was used to visualize inorganic nanoparticles in waste leachates [116]. A scanning unit can be installed to a TEM instrument (STEM), which resembles the operation of a scanning electron microscope (SEM). In SEM, a convergent electron beam is used for scanning areas in a raster motion. Several detectors are installed to capture electrons and x-rays following the interaction of the beam with the sample material. Secondary electron (SE) detectors may be used for high resolution topographical information, backscattered electron (BSE) detectors for elemental contrast, and energy dispersive x-ray spectroscopy (EDS or EDX) detectors for elemental composition. TEM detectors for higher resolution images and quantitative EDX analysis (STEM) may also be installed, but only on very thin samples (up to 1 µm). SEM is more appealing for application with environmental samples owing to the possibility of semi-automatic procedures supported by image analysis tools, which may be used to acquire morphological characteristics and qualitative particle composition, but not for quantitative composition and crystallography [115,117].

 Analysis of inorganic particles with SEM-EDX is possible when particles are deposited on a surface, which is a challenging task to accomplish without introducing artefacts. Alternatively, CryoTEM may be used, but this is an expensive and time-consuming solution that is typically avoided. A particle suspension is deposited on a surface, e.g. TEM grid, tape or membrane, and is allowed to dry. The water removed during drying reduces the distance between particles, thus enhancing the formation of agglomerates which were not present in suspension. An artificial corona on particles may also appear during sample preparation, due to changes in ion concentrations and pH during drying [118]. One solution is to remove the suspension, by means of a lint-free wipe, before the liquid volume is significantly reduced by drying. However, only the particles that attach on the surface during this time are analyzed further. An alternative is to add a suitable stabilizer in the suspension that prevents particle agglomeration [119]. Recently, the application of cloud point extraction treatment of environmental water samples prior to TEM-EDX analysis has shown promising results for metal-containing nanoparticles [120].

High vacuum is applied in the sample chamber to maintain stability of the electron beam, however under these conditions non-conductive samples will cause charging effects, thus distorting the acquired image. A conductive layer by means of sputtering is therefore applied on non-conductive materials. Because this layer is often not uniformly applied and will contribute to the EDX compositional analysis, an alternative is to conduct the analysis under variable pressure conditions, which is a promising tool for environmental and biological research [121]. The compositional information acquired with EDX is qualitative since the intensity of the detected characteristic x-rays depends on the interaction volume of the electron beam with the particle material. In turn, the interaction volume depends on the energy of the electron beam and the dimensions of the object examined. On smaller particles, the electrons will penetrate the particle and the support underneath, thus producing mixed signals from both the particle and support. Using STEM, it is possible to acquire semi-quantitative information on particles with thickness (dimension parallel to the electron beam) less than 1 μm.

Plastic particles may be analyzed with SEM-EDX, producing morphological and compositional information. The concentration of carbon is qualitatively determined; however, it is not possible to identify the type of polymer. SEM has been used to determine changes on the surface of plastic particles caused by weathering under environmentally relevant conditions [122]. Concentrations of human exposure to microplastic particles from bottled mineral water have been calculated using analysis with SEM-EDX [123]. The particles containing carbon were assumed to be plastics, however, since mineral water contains inorganic and organic particles as well, which also contain carbon (e.g. carbonate salts, microorganisms and their residues), their identification is questionable [124]. Moreover, studies that have used SEM to verify plastic particle concentrations based on topographical contrast and elemental composition derived number concentrations of questionable validity, since no determination of polymer structure was made to verify these results [123,125].

6. Particle tracking analysis and dynamic light scattering

556

557

558

559 560

561

562

563

564 565

566 567

568

569

570

571

572

573

574 575

576

577

578

579 580

581

582

583

584

585

586 587

588

589

590 591

592

593

594 595

596

597

598 599

600

601

602

603

Particle tracking analysis (PTA) and dynamic light scattering (DLS) are two often complementary quantitative techniques which are used to determine the hydrodynamic diameter of micron- and nanometer-sized particles (≈ 1 to 10^3 nm) in synthetic and filtered surface water samples [70,126-128] . PTA and DLS theory are based on the movement of particles suspended in a fluid as a result of the Brownian motion of the surrounding fluid molecules. In PTA, particles in the sample are inundated with light at a single wavelength and the movement of particles is visualized and tracked using a charged coupled device (CCD) camera. The hydrodynamic particle diameter is then calculated based on a relationship between particle size and the diffusion coefficient, typically using the Stokes-Einstein equation for spherical particles. DLS, on the other hand, measures the intensity of the light scattered by the suspended particles over time (10s to 100s of seconds). An autocorrelation function representing the rate of fluctuation of the intensity of the scattered light (due to particle motion) as a function of time is processed to obtain the diffusion coefficient (Brownian motion) of the particles and thus the particle diameter. With respect to additional particle characterization, DLS analyzers are often coupled with either an electrophoretic light scattering mode to measure particle electrophoretic mobility and zeta potential or a static light scattering mode to measure the radius of gyration, while PTA can quantify the particle number concentration, along with qualitative surface properties resulting from the interaction of the particle surface with light.

A major limitation of DLS is that smaller size fractions often remain undetected due to relatively higher light scattering by larger particles. As a bulk or ensemble measurement, conventional DLS is more sensitive to larger particles that can obscure the scattering signal of smaller particles in the population (Figure 5a), and hence intensity-weighted size distributions are most immediately derived from the autocorrelation function. On the other hand, PTA tracks single particles and is comparatively more sensitive to particles at the lower end of the size range, producing number-weighted size distributions (Figure 5b); however, there is room for improvement in PTA in terms of the detection limit (currently ~10 nm) and susceptibility to visualization artefacts [126,129]. Hence, DLS is better suited to monodisperse rather than polydisperse particle size distributions, while PTA performs well with monodisperse particle size distributions and better than DLS with polydisperse particle size distributions, though it still suffers from scattering errors in polydisperse suspensions [129]. A prefiltration step is often necessary to remove background signal from colloids in environmental samples. Another limitation is that there is an optimum range for the intensity of the scattered light that restricts the usable particle concentration range; the sample scattering must be sufficiently high to provide good signal-to-noise ratio [130] (e.g., for a background scattering of 10 kcps, sample scattering of > 20 kilo counts per second (kcps) or higher would be required). Neither technique performs well with highly concentrated particle suspensions, where particle interactions can influence the particle motion, and so sample dilution is often required.

To address the challenge of accurate particle size measurements in polydisperse samples, multiple approaches have been developed. For example, algorithms which deconvolute autocorrelation functions produced by polydisperse samples (e.g., CONTIN, CORENN) [131,132] and statistical models (e.g., MApNTA) [133] can be used to identify multiple particle size distributions in the same particle suspension. Data can also be averaged over shortened time intervals to identify, remove, and/or differentially analyze "unwanted" size fractions such as large dust impurities or aggregated particles [134]. Finally, multispectral PTA (m-PTA) utilizes several incident light wavelengths and allows for improved sensitivity of polydisperse particle distributions [129]. To address the challenge of size measurements for highly concentrated samples, approaches such as modulated 3D cross-correlation DLS [135,136], fiber optic quasi-elastic light scattering (FOQELS) [137,138], and ultrasonic attenuation spectroscopy [139–141] have been developed or are under development. Differences in the intensity of scattered light of aggregated particles and natural components using PTA have been utilized to study aggregation kinetics of nanoparticles in landfill leachates and natural seawater [142,143].

New directions in the particle sizing field include the use of single-particle DLS (SP-DLS) to identify the shapes of individual particles [144], though this technique is in its infancy. Image-based DLS (DLSI) [145], in which the intensity of the scattered light is imaged over time and in multiple space-dimensions, reduces the time required to obtain data compared to conventional DLS and improves the resolution of conventional DLS. DLSI has the potential to be applied to real-time flow through systems, possibly even in situ size characterization. The hyphenation of DLS with separation techniques such as field flow fractionation (FFF) has also been performed and provides a wider particle size range of detection.

7. Field flow fractionation

Field - flow fractionation (FFF) is a chromatographic method that is capable of separating macromolecular and particulate species, typically by size (Figure 5c) [146]. In FFF, the sample is injected into the FFF channel, and an applied force pushes the particles toward an "accumulation wall". Particles equilibrate at different distances from the accumulation wall depending on their properties or interaction with the applied force. The particles are then eluted under laminar flow pattern, with particles further from the accumulation wall experiencing higher flowrates and hence eluting earlier. The applied force can be established by a variety of means. Most typically, fluid cross flow (termed flow FFF) is applied using an ultrafiltration membrane as the accumulation wall. Flow FFF can further be categorized by the channel and cross flow configuration, with asymmetric flow FFF (AF4) performed with the membrane at the bottom of a flat channel, and hollow fiber FFF (HF-FFF) using a tubular membrane with radial cross flow. In flow FFF, particles are separated by their diffusion rate toward the center of the channel, with smaller particles residing further from the accumulation wall and eluting faster. Centrifugal FFF (termed centrifugal or sedimentation FFF, or CFFF) can also be used to separate particles by their buoyant force (size and density). Potential advantages of FFF over other size separation methods include the gentle nature of the separation and capability for separation over a continuous size distribution (as opposed to discrete size cutoffs). Coupling FFF with online detectors then produces size-resolved characterization of the nanoparticles.

Recent advances in FFF for nanoparticle analysis in environmental samples address challenges in both the *separation/sizing* and *compositional analysis*.

652653654

655

656

657

658 659

660

661 662

663

664 665

666

667 668

669 670

671

672 673

674

675

676

651

Environmental samples covering a wide size distribution pose challenges in FFF separation. For example, in AF4, the cross flow is typically held fixed, allowing optimal separation across only a relatively narrow size range, e.g. 1-100 nm. Recent studies have achieved separation across a broader size range by employing a variable cross flow profile, as demonstrated on carbon-based aggregates and nanoplastics in AF4 (separation across 1 to 800 nm) [147] and PS nanoparticles in frit inlet AF4 (separation across 50 nm to ~ 1 μm) [148]. Challenges remain in extending the size separation range beyond 1 µm. Above this size range, a transition from normal to "steric" elution mode occurs, where the large size of the particle prevents approach to the accumulation wall, such that larger particles experience faster flow rates and elute more quickly rather than more slowly. Hence, reliable size separation will not be achieved in polydisperse samples with sizes spanning the normal and steric elution modes, and preseparation, for example by centrifugation, would be required before AF4 analysis [149–151]. As the elution time can also be affected by the shape of the particle [152–154] and interactions with the accumulation wall, coupling FFF with online DLS or collecting fractions for offline characterization (e.g., by AFM [153], TEM [155], or SEM [156]) is important to directly measure sizes and shapes. Furthermore, the use of both online DLS and multi-angle or static light scattering (MALS or SLS) to compare the hydrodynamic radius and radius of gyration yields a shape factor that can be used to distinguish solid spheres from other structures (e.g., rods, core-shell structures, etc.) [157–161]. However, care must be taken to avoid errors in online DLS analysis if the particle concentrations are low [162] or the AF4 flow velocity is significant relative to the diffusion rate of the particles [163]. Recent advances in online sizing include the coupling of FFF with nanoparticle tracking analysis (NTA), as demonstrated on mixtures of different sizes of PS nanoplastics [164], which is advantageous for small particles that do not scatter as efficiently in DLS analysis.

677 678 679

680

681

682

683 684

685

686 687

688

689

690

691 692

693 694

695

696 697

698

699

700

Characterization of the composition of the fractionated particles also poses challenges, especially in natural samples. First, sensitivity can be a limiting factor, as the sample is diluted after injection in the FFF mobile phase and may show poor recovery from the channel [149,151]. Introducing surfactant in the mobile phase can minimize losses but may disrupt the natural aggregation state of the samples. Alternatively, higher sample masses can be injected using semi-preparative FFF [161,165]. Dilution can also be minimized by using HF-FFF instead of AF4 [166], or by splitting particle-free flow from the AF4 effluent, such that a more concentrated sample stream is sent to the detectors. The capability to quantify mass concentrations in the AF4 eluent, as well as the sensitivity and selectivity, will also depend on the choice and optimization of online detectors. In the most common online detectors (UV-Vis and light scattering), anthropogenic nanomaterials often do not show any distinguishing features from other natural colloids. UV detection is also prone to interferences from particle light scattering, which is disproportionally weighted to large particles. If heteroaggregates of anthropogenic and natural colloids are present, distinguishing the presence or size of the anthropogenic material will be even more challenging. To help overcome these issues, FFF has frequently been coupled with ICP-MS for selective and quantitative detection of anthropogenic nanoparticles in environmental samples containing natural colloids. For example, FFF-ICP-MS has been applied to detect TiO₂ and Ag nanoparticles in wastewater [167]. It has further been applied to identify individual nanoparticles and those heteroaggregated with soil or sediment colloids, for example for CdSe/ZnS quantum dots [168], Au NPs [169], and phosphorus (P) in black carbon [165]. Recent advances in FFF-ICP-MS include the use of TOF-ICP-MS to rapidly monitor multiple isotopes, enabling more comprehensive analysis of highly complex

mixtures of engineered and natural nanoparticles and colloids [88]. For nanoplastics, AF4 has been applied to collect size fractions for offline ICP-MS analysis of nanoplastics doped with Pd as a tracer [170]. AF4-ICP-MS and CFFF-ICP-MS have also been applied to characterize composite particles of metal nanoparticles within plastics [171]. These two modes produced complementary information: AF4 separated the composites by their overall hydrodynamic size, whereas the plastic matrix could be rendered "invisible" in CFFF by density-matching the mobile phase, resulting in separation by the number of metal nanoparticles per plastic. Another selective detection mode recently coupled to AF4 is magnetic particle spectroscopy for magnetic nanoparticles, such as iron-based biomedical imaging agents [172].

Online detection and identification of purely plastic or carbon-based nanoparticles is currently a major challenge in AF4 analysis, as AF4-ICP-MS does not provide information on the molecular composition of organic materials such as plastics. Light scattering has been explored as an AF4 detector to detect PS and PE nanoplastics in fish after enzymatic digestion; while the spiked PS could be detected, the PE nanoplastics were not distinguishable from the light scattering background of the fish digest [150]. Hence, more selective detectors are required. Herrero et al. coupled AF4 with atmospheric pressure photoionization (APPI) - Orbitrap mass spectrometry for identification of fullerene nanoparticles and aggregates [173]; however, this direct interfacing would not be well suited for larger nanoplastics. Schwaferts et al. have made a major recent advancement in hyphenating AF4 and centrifugal FFF with optical tweezers to concentrate the eluting nanoplastics followed by Raman detection to identify the plastics [46]; this method can hold great promise for nanoplastics analysis if the availability of the instrumentation is expanded. However, owing to the multiple conditions that can be adjusted, the method development of FFF techniques is a time-consuming process [174], which remains a major barrier for its broad utilization. Further improvement in detection capabilities and commercialization of accessories to directly couple them with AF4 will also be a critical area to expand the applicability of AF4.

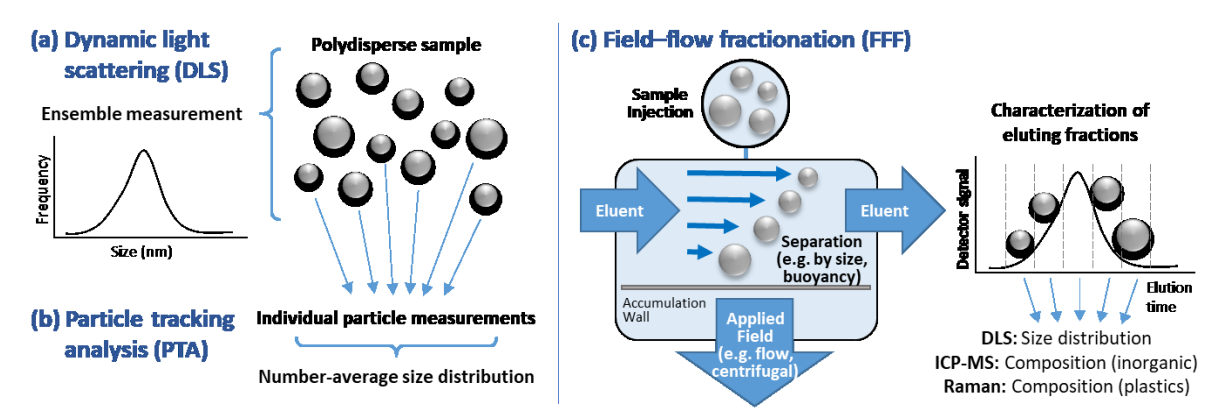


Figure 5. Particle sizing methods – dynamic light scattering (A) and particle tracking analysis (B), and field-flow fractionation (C) for particle separation with optional "hyphenation" to online detectors for size-resolved analysis.

8. Future perspectives

The release of anthropogenic particles to the environment is arguably one of the biggest concerns of societies and governments today worldwide due to the potential risks that these particles pose to human health and ecosystems. The complexity and abundance of anthropogenic particles increases toward the smallest size ranges (e.g., nanoscale), where

particles have lower mass but larger surface area available for mass transfer and surface reactions and are more likely to be ingested by animals, especially invertebrates that are in the lower trophic levels of the food chain. To adequately address the questions of human health and ecosystem risks, analytical methods must be used which provide particle number, size, mass and composition data at increasingly small scales and levels of complexity. However, sample preparation and analytical methods for particle identification are more established for microparticles, while to some extent there is still a methodological gap for nanoparticles. This gap hinders the progress to universally understand the source, fate, and effects of nanoparticles in the environment; hence, one of the future directions in this field is to fulfill this research gap by developing and improving methods and techniques for nanoparticles analysis, as demonstrated in Figure 6.

Surface Area Mass of particles Ingestion risk Sample processing Number of particles Future goal Analytical Methods

Anthropogenic Particles

Figure 6. Schematic representation of the relative importance of anthropogenic particle features in nano and micro scale (top four bars), including the current state of development and anticipated future direction of analytical methods (figure adapted from [175])

 $1 \mu m$

Micro

5 mm

ENM < 100 μm

Nano

In this review, advances in several analytical methods with these capabilities are discussed. However, there are still challenges such as sampling harmonization, analytical identification, and data processing which, if addressed, can significantly improve data quality and reproducibility, resolution, and representativeness (Table 1). Harmonization efforts such as standardization of reference materials, methods and sample processing protocols and the development of shared databases for data analysis and interpretation are sorely needed in order to provide reliable and comparable results across laboratories. For instance, vibrational spectroscopy is one of the most advanced and commonly used technique for microplastic identification, but development is still needed in the direction of data processing and validation. For inorganic particles on the other hand, methods such as spICPMS and SEM-EDX call for further development in data management and processing, in addition to validation and

standardization of sample handling protocols. Moreover, for all methods discussed, there is a need for development to increase throughput with standardized and automated systems and to expand the limit of detection or separation to broader size ranges. Miniaturization is also expected to play a critical role in enabling field applications and thus facilitating monitoring efforts.

Other foreseeable future analytical directions include the maturation of semi-quantitative aspects of the various techniques and further development of hyphenated techniques, particularly combining new techniques targeting nanoparticles of emerging concern, including plastics, paint flakes, TRWP, engineered nanomaterials. Some of the techniques discussed produce semi-quantitative data, e.g., from a two-dimensional image it is possible to estimate the particle mass if the thickness of the particle is also assumed and its chemical composition and density are known. Similarly, spICPMS results can be used to derive particle size distribution by making assumptions on the density, composition, and shape of the particles. Hyphenation of techniques has provided significant leaps forward for particle analysis. For example, the current state-of-the-art for microplastic analysis is μ-FTIR and μ-Raman, i.e. the combination of microscopy with a spectrometer, where chemical composition can be obtained in combination with two-dimensional size distribution and number of imaged particles. For example, Mattsson et al. used a combination of techniques including FTIR, Raman, SEM, and NTA to study environmental weathering of expanded polystyrene particles covering a size range from 0.01 to 1,000 µm [176]. Similarly, Py-GCMS is a combination of techniques providing chemical composition and masses of particles in both the micro- and nanoscale. New combinations such as FFF coupled to optical tweezers and Raman spectroscopy are only recently being developed for analysis of emerging anthropogenic particles such as plastics, paint, tire wear and road particles. All these hyphenated methods produce multi-dimensional data sets (e.g., size- or spatially resolved spectra), and software tools need to be developed for automated data integration and visualization.

Acknowledgements

768

769

770

771772

773

774

775776

777

778

779780

781

782 783

784 785

786

787 788

789

790

791 792

793

794 795 796

797

798

799

800 801

806 807

808 809 810

811

812813814815

AG was supported by the NanoIsland project, financed by the Hellenic Foundation for Research and Innovation (HFRI) and the General Secretariat for Research and Technology (GSRT), under grant agreement No. 1317 AD was supported by the Texas Tech University Whitacre College of Engineering. SL was supported by U.S. Department of Agriculture under Grant No. 2018-67022-27969 (PSGT#17545), U.S. National Science Foundation (no. 1705511). KM was supported by the Swedish EPA. VHS was supported by Aarhus University.

Declaration of interests

X The authors declare that they have no known competing financial interests or personal relationships that could have appeared to influence the work reported in this paper.

Author contribution

KM and AG conceived the idea and drafted the outline. All authors wrote the manuscript. All authors discussed, reviewed, edited, and approved the manuscript.

Table 1. Overview of the most common analytical techniques for anthropogenic analysis of nano- and microparticles.

Technique	Analytical information	Size or mass concentrati on limit of detection	Advantages	Limitation	Analytical information	General remarks	Applicable materials
μ-FTIR Transmittance Reflectance	Chemical fingerprint.	< 10 μm	Sample Mapping. Sample Mapping.	Particle thick. >300μm. Reflective error.	Chemical fingerprint.	Particle morphology can display spectral interferences mostly in reflectance and ATR measurements. Reflective crystal must be in full contact with the particle for ATR measurements.	Microplastics
ATR		< Reflective Crystal Size	Lower detection limit.	Not suitable for mapping.		High interference from water signal.	
Confocal Raman	Chemical fingerprint.	< 1 μm	Low interference from water signal. Less sensitive for degradation. Aqueous samples.	Fluorescence signal. Weak signal. Might burn the sample.	Chemical fingerprint.	Sample mapping or particle measurements is still time consuming.	Microplastics
Py-CG/MS	Mass concentratio n, polymer identificatio n and particle composition.	< 1 μg	Whole particle analysis. Quantitative analysis (mass). Differentiation between plastic polymers and organic additives. Low mass detection limit.	Destructive technique. Only information about organic compounds.	Mass concentration. Polymer identification. Particle composition.	Complementary to Raman and FTIR spectroscopies. Appropriate sample pre-treatment may be needed for removal of potential environmental or biological matrix interferences.	Micro-nanoplastics, TRWP

FFF	Size fractionation	< 1 nm	Relatively gentle (aqueous) sample separation across continuous size distribution . Can be coupled with various detectors for sizing and compositional analysis	Low sample injection volume, high sample dilution, or low recovery in analytical FFF mode may result in low sensitivity.	Size fractionation, size distribution, and composition (with online detection, or fraction collection with offline analysis)	Sample pretreatment may be needed to separate < 1 µm and > 1 µm particles that elute in normal and steric elution mode, respectively. Surfactants may need to be added to achieve higher sample recovery	Nanoplastics, ENMs, Microparticles
PTA	Particle concentratio n and size distribution.	< 10 nm	High throughput and easy to use. Low limit of detection for particle size. Performs better with polydisperse samples compared to DLS.	Visualization artefacts. Poor performance with highly concentrated samples. No chemical composition data	Particle concentration and size distribution.	Provides particle number concentration. Complementary to DLS.	Nanoplastics, ENMs, soot, TRWP
DLS	Particle size distribution and particle properties (zetapotentia l, electrophore tic mobility)	< 10 nm	User friendly. High throughput and short analysis time. Low limit of detection for particle size.	Skewed towards larger particle sizes. Not useful as a standalone technique in polydisperse and highly concentrated samples. No chemical composition data	Particle size distribution and particle properties (zetapotential, electrophoretic mobility).	Provides data on electrophoretic mobility and zetapotential. Complementary to PTA.	Nanoplastics, ENMs, soot, TRWP
SEM-EDX	Size, shape, number and composition of particles	< 100 nm	Holistic analysis includes number, size, shape, and composition, applicable on a wide range of particle sizes.	Sample preparation artefacts, qualitative or semi-quantitative composition.	Size, shape, number and composition of particles	Careful sample preparation in contamination- free environment is necessary. The analytical process is time consuming (low throughput)	ENMs, soot
spICPMS	Particle concentratio n and estimation of size distribution	< 10 nm	High throughput analysis, low limits of detection, mature technology with a variety of solutions available for most issues.	Scarcity of properly characterized and stable reference materials, complex and developing data analysis, destructive technique	Particle concentration and estimation of size distribution	Composition, shape, and density assumptions to derive size distribution necessitate use of complementary techniques.	ENMs, microplastics

- Hartmann NB, Hüffer T, Thompson RC, Hassellöv M, Verschoor A, Daugaard AE, et al. Are We Speaking the Same Language? Recommendations for a Definition and Categorization Framework for Plastic Debris. Environ Sci Technol 2019;53:1039–47. https://doi.org/10.1021/acs.est.8b05297.
- Auffan M, Rose J, Bottero J-Y, Lowry G V, Jolivet J-P, Wiesner MR. Towards a definition of inorganic nanoparticles from an environmental, health and safety perspective. Nat Nanotechnol 2009;4:634–41. https://doi.org/10.1038/nnano.2009.242.
- Allen S, Allen D, Phoenix VR, Le Roux G, Durántez Jiménez P, Simonneau A, et al.
 Atmospheric transport and deposition of microplastics in a remote mountain
 catchment. Nat Geosci 2019;12:339–44. https://doi.org/10.1038/s41561-019-0335-5.
- Wang W, Yuan W, Chen Y, Wang J. Microplastics in surface waters of Dongting Lake
 and Hong Lake, China. Sci Total Environ 2018;633:539–45.
 https://doi.org/10.1016/j.scitotenv.2018.03.211.
- 834 [5] Cózar A, Echevarría F, González-Gordillo JI, Irigoien X, Úbeda B, Hernández-León S,
 835 et al. Plastic debris in the open ocean. Proc Natl Acad Sci U S A 2014;111:10239–44.
 836 https://doi.org/10.1073/pnas.1314705111.
- shan J, Zhao J, Liu L, Zhang Y, Wang X, Wu F. A novel way to rapidly monitor microplastics in soil by hyperspectral imaging technology and chemometrics. Environ Pollut 2018;238:121–9. https://doi.org/10.1016/j.envpol.2018.03.026.
- Haave M, Lorenz C, Primpke S, Gerdts G. Different stories told by small and large microplastics in sediment first report of microplastic concentrations in an urban recipient in Norway. Mar Pollut Bull 2019;141:501–13. https://doi.org/10.1016/j.marpolbul.2019.02.015.
- Lusher AL, O'Donnell C, Officer R, O'Connor I. Microplastic interactions with North
 Atlantic mesopelagic fish. ICES J Mar Sci 2016;73:1214–25.
 https://doi.org/10.1093/icesjms/fsv241.
- Wang D, Su L, Ruan HD, Chen J, Lu J, Lee CH, et al. Quantitative and qualitative determination of microplastics in oyster, seawater and sediment from the coastal areas in Zhuhai, China. Mar Pollut Bull 2021;164:112000.

 https://doi.org/10.1016/j.marpolbul.2021.112000.
- 851 [10] Souza VGL, Fernando AL. Nanoparticles in food packaging: Biodegradability and potential migration to food-A review. Food Packag Shelf Life 2016;8:63–70. https://doi.org/10.1016/j.fpsl.2016.04.001.
- Ragusa A, Svelato A, Santacroce C, Catalano P, Notarstefano V, Carnevali O, et al.
 Plasticenta: First evidence of microplastics in human placenta. Environ Int
 2021;146:106274. https://doi.org/10.1016/j.envint.2020.106274.
- Buffle J, van Leeuwen HP, McCarthy JF. Sampling and Characterization of Colloids
 and Particles in Groundwater for Studying their Role in Contaminant Transport.
 Environ. Part., CRC Press; 2019, p. 247–315. https://doi.org/10.1201/9781351270809-6.
- 861 [13] Mattsson K, Johnson E V., Malmendal A, Linse S, Hansson LA, Cedervall T. Brain damage and behavioural disorders in fish induced by plastic nanoparticles delivered through the food chain. Sci Rep 2017;7:1–7. https://doi.org/10.1038/s41598-017-10813-0.
- 865 [14] Salzer R, Siesler HW. Infrared and Raman Spectroscopic Imaging. 2nd ed. John Wiley & Sons, Inc.; 2014.
- 867 [15] Xu JL, Thomas K V., Luo Z, Gowen AA. FTIR and Raman imaging for microplastics

- analysis: State of the art, challenges and prospects. TrAC Trends Anal Chem 2019;119:115629. https://doi.org/10.1016/j.trac.2019.115629.
- Renner G, Schmidt TC, Schram J. Characterization and Quantification of Microplastics
 by Infrared Spectroscopy. Compr Anal Chem 2017;75:67–118.
 https://doi.org/10.1016/bs.coac.2016.10.006.
- [17] Dougan JA, Chan KLA, Kazarian SG. FT-IR Imaging in ATR and Transmission
 Modes: Practical Considerations and Emerging Applications. Infrared Raman
 Spectrosc. Imaging, vol. 9783527336524, Weinheim, Germany: Wiley-VCH Verlag
 GmbH & Co. KGaA; 2014, p. 397–444. https://doi.org/10.1002/9783527678136.ch9.
- Primpke S, Lorenz C, Rascher-Friesenhausen R, Gerdts G. An automated approach for microplastics analysis using focal plane array (FPA) FTIR microscopy and image analysis. Anal Methods 2017;9:1499–511. https://doi.org/10.1039/c6ay02476a.
- Primpke S, Godejohann M, Gerdts G. Rapid Identification and Quantification of Microplastics in the Environment by Quantum Cascade Laser-Based Hyperspectral Infrared Chemical Imaging. Environ Sci Technol 2020;54:15893–903. https://doi.org/10.1021/acs.est.0c05722.
- 884 [20] Meyns M, Primpke S, Gerdts G. Library based identification and characterisation of 885 polymers with nano-FTIR and IR-sSNOM imaging. Anal Methods 2019;11:5195–202. 886 https://doi.org/10.1039/c9ay01193e.
- 887 [21] Schnell M, Goikoetxea M, Amenabar I, Carney PS, Hillenbrand R. Rapid Infrared 888 Spectroscopic Nanoimaging with nano-FTIR Holography. ACS Photonics 889 2020;7:2878–85. https://doi.org/10.1021/acsphotonics.0c01164.
- Huth F, Govyadinov A, Amarie S, Nuansing W, Keilmann F, Hillenbrand R. Nano FTIR absorption spectroscopy of molecular fingerprints at 20 nm spatial resolution.
 Nano Lett 2012;12:3973–8. https://doi.org/10.1021/nl301159v.
- Eincinelli A, Scopetani C, Chelazzi D, Martellini T, Pogojeva M, Slobodnik J.
 Microplastics in the Black Sea sediments. Sci Total Environ 2021;760.
 https://doi.org/10.1016/j.scitotenv.2020.143898.
- Liu F, Vianello A, Vollertsen J. Retention of microplastics in sediments of urban and highway stormwater retention ponds. Environ Pollut 2019;255:113335.
 https://doi.org/10.1016/j.envpol.2019.113335.
- Käppler A, Fischer M, Scholz-Böttcher BM, Oberbeckmann S, Labrenz M, Fischer D, et al. Comparison of μ-ATR-FTIR spectroscopy and py-GCMS as identification tools for microplastic particles and fibers isolated from river sediments. Anal Bioanal Chem 2018;410:5313–27. https://doi.org/10.1007/s00216-018-1185-5.
- [26] Kirstein I V., Hensel F, Gomiero A, Iordachescu L, Vianello A, Wittgren HB, et al.
 Drinking plastics? Quantification and qualification of microplastics in drinking water
 distribution systems by μFTIR and Py-GCMS. Water Res 2021;188:116519.
 https://doi.org/10.1016/j.watres.2020.116519.
- 907 [27] Suteja Y, Atmadipoera AS, Riani E, Nurjaya IW, Nugroho D, Cordova MR. Spatial 908 and temporal distribution of microplastic in surface water of tropical estuary: Case 909 study in Benoa Bay, Bali, Indonesia. Mar Pollut Bull 2021;163:111979. 910 https://doi.org/10.1016/j.marpolbul.2021.111979.
- 911 [28] Vinay Kumar BN, Löschel LA, Imhof HK, Löder MGJ, Laforsch C. Analysis of 912 microplastics of a broad size range in commercially important mussels by combining 913 FTIR and Raman spectroscopy approaches. Environ Pollut 2021;269:116147. 914 https://doi.org/10.1016/j.envpol.2020.116147.
- 915 [29] Borman SA. Nonlinear Raman Spectroscopy. Anal Chem 1982;54:1021–6. 916 https://doi.org/10.1021/ac00246a002.
- 917 [30] Dieing T, Hollricher O, Toporski J. Confocal Raman Microscopy. vol. 158. 2010.

- 918 https://doi.org/10.1007/978-3-642-12522-5.
- [31] Wolff S, Kerpen J, Prediger J, Barkmann L, Müller L. Determination of the microplastics emission in the effluent of a municipal waste water treatment plant using
 Raman microspectroscopy. Water Res X 2019;2:100014.
 https://doi.org/10.1016/j.wroa.2018.100014.
- 923 [32] Di M, Wang J. Microplastics in surface waters and sediments of the Three Gorges
 924 Reservoir, China. Sci Total Environ 2018;616–617:1620–7.
 925 https://doi.org/10.1016/j.scitotenv.2017.10.150.
- [33] Liu J, Zhang X, Du Z, Luan Z, Li L, Xi S, et al. Application of confocal laser Raman
 spectroscopy on marine sediment microplastics. J Oceanol Limnol 2020;38:1502–16.
 https://doi.org/10.1007/s00343-020-0129-z.
- 929 [34] Oßmann BE, Sarau G, Holtmannspötter H, Pischetsrieder M, Christiansen SH, Dicke
 930 W. Small-sized microplastics and pigmented particles in bottled mineral water. Water
 931 Res 2018;141:307–16. https://doi.org/10.1016/j.watres.2018.05.027.
- 932 [35] Pittroff M, Müller YK, Witzig CS, Scheurer M, Storck FR, Zumbülte N. Microplastic 933 analysis in drinking water based on fractionated filtration sampling and Raman 934 microspectroscopy. Environ Sci Pollut Res 2021. https://doi.org/10.1007/s11356-021-935 12467-y.
- [36] Langer J, de Aberasturi DJ, Aizpurua J, Alvarez-Puebla RA, Auguié B, Baumberg JJ,
 et al. Present and future of surface-enhanced Raman scattering. ACS Nano
 2020;14:28–117. https://doi.org/10.1021/acsnano.9b04224.
- [37] Halvorson RA, Vikesland PJ. Surface-enhanced Raman spectroscopy (SERS) for
 environmental analyses. Environ Sci Technol 2010;44:7749–55.
 https://doi.org/10.1021/es101228z.
- [38] Lv L, He L, Jiang S, Chen J, Zhou C, Qu J, et al. In situ surface-enhanced Raman
 spectroscopy for detecting microplastics and nanoplastics in aquatic environments. Sci
 Total Environ 2020;728. https://doi.org/10.1016/j.scitotenv.2020.138449.
- Yu G, Cheng H, Jones R, Feng Y, Gong K, Li K, et al. Surface-Enhanced Raman
 Spectroscopy Facilitates the Detection of Microplastics <1 μm in the Environment.
 Environ Sci Technol 2020;54:15594–603. https://doi.org/10.1021/acs.est.0c02317.
- Zada L, Leslie HA, Vethaak AD, Tinnevelt GH, Jansen JJ, de Boer JF, et al. Fast
 microplastics identification with stimulated Raman scattering microscopy. J Raman
 Spectrosc 2018;49:1136–44. https://doi.org/10.1002/jrs.5367.
- 954 [42] Schmidt U, Hild S, Ibach W, Hollricher O. Characterization of Thin Polymer Films on 955 the Nanometer Scale with Confocal Raman AFM. Macromol Symp 2005;230:133–43. 956 https://doi.org/10.1002/masy.200551152.
- 957 [43] Webster S, Smith DA, Batchelder DN. Raman microscopy using a scanning near-field 958 optical probe. Vib Spectrosc 1998;18:51–9. https://doi.org/10.1016/s0924-959 2031(98)00037-x.
- Zhang W, Dong Z, Zhu L, Hou Y, Qiu Y. Direct Observation of the Release of
 Nanoplastics from Commercially Recycled Plastics with Correlative Raman Imaging
 and Scanning Electron Microscopy. ACS Nano 2020;14:7920–6.
 https://doi.org/10.1021/acsnano.0c02878.
- [45] Gillibert R, Balakrishnan G, Deshoules Q, Tardivel M, Magazzù A, Donato MG, et al.
 Raman tweezers for small microplastics and nanoplastics identification in seawater.
 Environ Sci Technol 2019;53:9003–13. https://doi.org/10.1021/acs.est.9b03105.
- 967 [46] Schwaferts C, Sogne V, Welz R, Meier F, Klein T, Niessner R, et al. Nanoplastic

- Analysis by Online Coupling of Raman Microscopy and Field-Flow Fractionation
 Enabled by Optical Tweezers. Anal Chem 2020;92:5813–20.
 https://doi.org/10.1021/acs.analchem.9b05336.
- 971 [47] Sobhani Z, Zhang X, Gibson C, Naidu R, Megharaj M, Fang C. Identification and visualisation of microplastics/nanoplastics by Raman imaging (i): Down to 100 nm. Water Res 2020;174:115658. https://doi.org/10.1016/j.watres.2020.115658.
- 974 [48] Fang C, Sobhani Z, Zhang X, Gibson CT, Tang Y, Naidu R. Identification and visualisation of microplastics/ nanoplastics by Raman imaging (ii): Smaller than the diffraction limit of laser? Water Res 2020;183:116046.
 977 https://doi.org/10.1016/j.watres.2020.116046.
- Fang C, Sobhani Z, Zhang X, McCourt L, Routley B, Gibson CT, et al. Identification and visualisation of microplastics / nanoplastics by Raman imaging (iii): algorithm to cross-check multi-images. Water Res 2021;194:116913.

 https://doi.org/10.1016/j.watres.2021.116913.
- 982 [50] Primpke S, Dias PA, Gerdts G. Automated identification and quantification of microfibres and microplastics. Anal Methods 2019;11:2138–47. 984 https://doi.org/10.1039/c9ay00126c.
- 985 [51] Munno K, De Frond H, O'donnell B, Rochman CM. Increasing the Accessibility for Characterizing Microplastics: Introducing New Application-Based and Spectral Libraries of Plastic Particles (SLoPP and SLoPP-E). Anal Chem 2020;92:2443–51. https://doi.org/10.1021/acs.analchem.9b03626.
- 989 [52] Primpke S, Wirth M, Lorenz C, Gerdts G. Reference database design for the automated 990 analysis of microplastic samples based on Fourier transform infrared (FTIR) 991 spectroscopy. Anal Bioanal Chem 2018;410:5131–41. https://doi.org/10.1007/s00216-992 018-1156-x.
- Primpke S, Cross RK, Mintenig SM, Simon M, Vianello A, Gerdts G, et al. Toward the
 Systematic Identification of Microplastics in the Environment: Evaluation of a New
 Independent Software Tool (siMPle) for Spectroscopic Analysis. Appl Spectrosc
 2020;74:1127–38. https://doi.org/10.1177/0003702820917760.
- Wander L, Vianello A, Vollertsen J, Westad F, Braun U, Paul A. Exploratory analysis of hyperspectral FTIR data obtained from environmental microplastics samples. Anal Methods 2020;12:781–91. https://doi.org/10.1039/c9ay02483b.
- Hufnagl B, Steiner D, Renner E, Löder MGJ, Laforsch C, Lohninger H. A
 methodology for the fast identification and monitoring of microplastics in
 environmental samples using random decision forest classifiers. Anal Methods
 2019;11:2277–85. https://doi.org/10.1039/c9ay00252a.
- 1004 [56] Renner G, Sauerbier P, Schmidt TC, Schram J. Robust Automatic Identification of Microplastics in Environmental Samples Using FTIR Microscopy. Anal Chem 2019;91:9656–64. https://doi.org/10.1021/acs.analchem.9b01095.
- Da Silva VH, Murphy F, Amigo JM, Stedmon C, Strand J. Classification and Quantification of Microplastics (<100 μm) Using a Focal Plane Array-Fourier
 Transform Infrared Imaging System and Machine Learning. Anal Chem
 2020;92:13724–33. https://doi.org/10.1021/acs.analchem.0c01324.
- 1011 [58] Hermabessiere L, Himber C, Boricaud B, Kazour M, Amara R, Cassone AL, et al.
 1012 Optimization, performance, and application of a pyrolysis-GC/MS method for the
 1013 identification of microplastics. Anal Bioanal Chem 2018;410:6663–76.
 1014 https://doi.org/10.1007/s00216-018-1279-0.
- 1015 [59] Nuelle MT, Dekiff JH, Remy D, Fries E. A new analytical approach for monitoring microplastics in marine sediments. Environ Pollut 2014;184:161–9. https://doi.org/10.1016/j.envpol.2013.07.027.

- 1018 [60] Dierkes G, Lauschke T, Becher S, Schumacher H, Földi C, Ternes T. Quantification of microplastics in environmental samples via pressurized liquid extraction and pyrolysis-gas chromatography. Anal Bioanal Chem 2019;411:6959–68.

 1021 https://doi.org/10.1007/s00216-019-02066-9.
- 1022 [61] Fries E, Dekiff JH, Willmeyer J, Nuelle MT, Ebert M, Remy D. Identification of polymer types and additives in marine microplastic particles using pyrolysis-GC/MS and scanning electron microscopy. Environ Sci Process Impacts 2013;15:1949–56. https://doi.org/10.1039/c3em00214d.
- 1026 [62] Dehaut A, Cassone AL, Frère L, Hermabessiere L, Himber C, Rinnert E, et al.
 1027 Microplastics in seafood: Benchmark protocol for their extraction and characterization.
 1028 Environ Pollut 2016;215:223-33. https://doi.org/10.1016/j.envpol.2016.05.018.
- Fischer M, Scholz-Böttcher BM. Simultaneous Trace Identification and Quantification of Common Types of Microplastics in Environmental Samples by Pyrolysis-Gas
 Chromatography-Mass Spectrometry. Environ Sci Technol 2017;51:5052–60.
 https://doi.org/10.1021/acs.est.6b06362.
- 1033 [64] Unice KM, Kreider ML, Panko JM. Comparison of tire and road wear particle
 1034 concentrations in sediment for watersheds in France, Japan, and the United States by
 1035 quantitative pyrolysis GC/MS analysis. Environ Sci Technol 2013;47:8138–47.
 1036 https://doi.org/10.1021/es400871j.
- Eisentraut P, Dümichen E, Ruhl AS, Jekel M, Albrecht M, Gehde M, et al. Two Birds with One Stone Fast and Simultaneous Analysis of Microplastics: Microparticles
 Derived from Thermoplastics and Tire Wear. Environ Sci Technol Lett 2018;5:608–13. https://doi.org/10.1021/acs.estlett.8b00446.
- 1041 [66] Panko JM, Chu J, Kreider ML, Unice KM. Measurement of airborne concentrations of tire and road wear particles in urban and rural areas of France, Japan, and the United States. Atmos Environ 2013;72:192–9. https://doi.org/10.1016/j.atmosenv.2013.01.040.
- 1045 [67] Ribeiro F, Okoffo ED, O'Brien JW, Fraissinet-Tachet S, O'Brien S, Gallen M, et al.
 1046 Quantitative Analysis of Selected Plastics in High-Commercial-Value Australian
 1047 Seafood by Pyrolysis Gas Chromatography Mass Spectrometry. Environ Sci Technol
 1048 2020;54:9408–17. https://doi.org/10.1021/acs.est.0c02337.
- 1049 [68] Li J, Liu H, Paul Chen J. Microplastics in freshwater systems: A review on occurrence,
 1050 environmental effects, and methods for microplastics detection. Water Res
 1051 2018;137:362-74. https://doi.org/10.1016/j.watres.2017.12.056.
- 1052 [69] Ivleva NP, Wiesheu AC, Niessner R. Microplastic in Aquatic Ecosystems. Angew Chemie Int Ed 2017;56:1720–39. https://doi.org/10.1002/anie.201606957.
- Ter Halle A, Jeanneau L, Martignac M, Jardé E, Pedrono B, Brach L, et al. Nanoplastic in the North Atlantic Subtropical Gyre. Environ Sci Technol 2017;51:13689–97.
 https://doi.org/10.1021/acs.est.7b03667.
- 1057 [71] Cole M, Webb H, Lindeque PK, Fileman ES, Halsband C, Galloway TS. Isolation of
 1058 microplastics in biota-rich seawater samples and marine organisms. Sci Rep 2014;4:1–
 1059 8. https://doi.org/10.1038/srep04528.
- 1060 [72] Mintenig SM, Int-Veen I, Löder MGJ, Primpke S, Gerdts G. Identification of
 1061 microplastic in effluents of waste water treatment plants using focal plane array-based
 1062 micro-Fourier-transform infrared imaging. Water Res 2017;108:365–72.
 1063 https://doi.org/10.1016/j.watres.2016.11.015.
- 1064 [73] Claessens M, Van Cauwenberghe L, Vandegehuchte MB, Janssen CR. New techniques 1065 for the detection of microplastics in sediments and field collected organisms. Mar 1066 Pollut Bull 2013;70:227–33. https://doi.org/10.1016/j.marpolbul.2013.03.009.
- 1067 [74] Collard F, Gilbert B, Eppe G, Parmentier E, Das K. Detection of Anthropogenic

- Particles in Fish Stomachs: An Isolation Method Adapted to Identification by Raman Spectroscopy. Arch Environ Contam Toxicol 2015;69:331–9. https://doi.org/10.1007/s00244-015-0221-0.
- 1071 [75] Vandermeersch G, Van Cauwenberghe L, Janssen CR, Marques A, Granby K, Fait G, et al. A critical view on microplastic quantification in aquatic organisms. Environ Res 2015;143:46–55. https://doi.org/10.1016/j.envres.2015.07.016.
- 1074 [76] Unice KM, Kreider ML, Panko JM. Use of a deuterated internal standard with
 1075 pyrolysis-GC/MS dimeric marker analysis to quantify tire tread particles in the
 1076 environment. Int J Environ Res Public Health 2012;9:4033–55.
 1077 https://doi.org/10.3390/ijerph9114033.
- 1078 [77] Shin T, Hajime O, Chuichi W. Pyrolysis–GC/MS Data Book of Synthetic Polymers. 1079 Elsevier B.V.; 2011.
- 1080 [78] Snyder DT, Pulliam CJ, Ouyang Z, Cooks RG. Miniature and Fieldable Mass
 1081 Spectrometers: Recent Advances. Anal Chem 2016;88:2–29.
 1082 https://doi.org/10.1021/acs.analchem.5b03070.
- Zhang X, Zhang H, Yu K, Li N, Liu Y, Liu X, et al. Rapid Monitoring Approach for Microplastics Using Portable Pyrolysis-Mass Spectrometry. Anal Chem
 2020;92:4656–62. https://doi.org/10.1021/acs.analchem.0c00300.
- 1086 [80] Montaño MD, Olesik JW, Barber AG, Challis K, Ranville JF. Single Particle ICP-MS:
 1087 Advances toward routine analysis of nanomaterials. Anal Bioanal Chem
 1088 2016;408:5053-74. https://doi.org/10.1007/s00216-016-9676-8.
- 1089 [81] Lee S, Bi X, Reed RB, Ranville JF, Herckes P, Westerhoff P. Nanoparticle size detection limits by single particle ICP-MS for 40 elements. Environ Sci Technol 2014;48:10291–300. https://doi.org/10.1021/es502422v.
- Hetzer B, Burcza A, Gräf V, Walz E, Greiner R. Online-coupling of AF4 and single particle-ICP-MS as an analytical approach for the selective detection of nanosilver release from model food packaging films into food simulants. Food Control 2017;80:113–24. https://doi.org/10.1016/j.foodcont.2017.04.040.
- 1096 [83] Huynh KA, Siska E, Heithmar E, Tadjiki S, Pergantis SA. Detection and
 1097 Quantification of Silver Nanoparticles at Environmentally Relevant Concentrations
 1098 Using Asymmetric Flow Field-Flow Fractionation Online with Single Particle
 1099 Inductively Coupled Plasma Mass Spectrometry. Anal Chem 2016.
 1100 https://doi.org/10.1021/acs.analchem.6b00764.
- Zahira E Herrera R, Marina B, Anna K U, Hans JP M, Ruud JB P. Detection of
 Agglomerates Using Hydrodynamic Chromatography Hyphenated with Single Particle
 Inductively Coupled Plasma Mass Spectrometry. Curr Trends Anal Bioanal Chem
 2018;2. https://doi.org/10.36959/525/443.
- Hachenberger YU, Rosenkranz D, Kriegel FL, Krause B, Matschaß R, Reichardt P, et
 al. Tackling Complex Analytical Tasks: An ISO/TS-Based Validation Approach for
 Hydrodynamic Chromatography Single Particle Inductively Coupled Plasma Mass
 Spectrometry. Materials (Basel) 2020;13:1447. https://doi.org/10.3390/ma13061447.
- 1109 [86] Franze B, Strenge I, Engelhard C. Separation and detection of gold nanoparticles with capillary electrophoresis and ICP-MS in single particle mode (CE-SP-ICP-MS). J Anal At Spectrom 2017;32:1481–9. https://doi.org/10.1039/c7ja00040e.
- 1112 [87] Praetorius A, Gundlach-Graham A, Goldberg E, Fabienke W, Navratilova J, Gondikas 1113 A, et al. Single-particle multi-element fingerprinting (spMEF) using inductively-
- 1114 coupled plasma time-of-flight mass spectrometry (ICP-TOFMS) to identify engineered
- nanoparticles against the elevated natural background in soils. Environ Sci Nano 2017;4. https://doi.org/10.1039/c6en00455e.
- 1117 [88] Meili-Borovinskaya O, Meier F, Drexel R, Baalousha M, Flamigni L, Hegetschweiler

- A, et al. Analysis of complex particle mixtures by asymmetrical flow field-flow fractionation coupled to inductively coupled plasma time-of-flight mass spectrometry.

 J Chromatogr A 2021;1641:461981. https://doi.org/10.1016/j.chroma.2021.461981.
- 1121 [89] Tharaud M, Gondikas A, Benedetti M, von der Kammer F, Hofmann T, Cornelis G.
 1122 TiO2 nanomaterial detection in calcium rich matrices by spICPMS. A matter of resolution and treatment. J Anal At Spectrom 2017. https://doi.org/10.1039/c7ja00060j.
- 1124 [90] Bolea-Fernandez E, Leite D, Rua-Ibarz A, Balcaen L, Aramendía M, Resano M, et al.
 1125 Characterization of SiO2 nanoparticles by single particle-inductively coupled plasma1126 tandem mass spectrometry (SP-ICP-MS/MS). J Anal At Spectrom 2017;32:2140–52.
 1127 https://doi.org/10.1039/c7ja00138j.
- 1128 [91] Cornelis G, Hassellöv M. A signal deconvolution method to discriminate smaller 1129 nanoparticles in single particle ICP-MS. J Anal At Spectrom 2014;29:134–44. 1130 https://doi.org/10.1039/C3JA50160D.
- 1131 [92] Mozhayeva D, Engelhard C. A quantitative nanoparticle extraction method for microsecond time resolved single-particle ICP-MS data in the presence of a high background. J Anal At Spectrom 2019;34:1571–80.

 https://doi.org/10.1039/c9ja00042a.
- 1135 [93] Bolea-Fernandez E, Rua-Ibarz A, Velimirovic M, Tirez K, Vanhaecke F. Detection of microplastics using inductively coupled plasma-mass spectrometry (ICP-MS) operated in single-event mode. J Anal At Spectrom 2020;35:455–60. https://doi.org/10.1039/c9ja00379g.
- 1139 [94] Laborda F, Trujillo C, Lobinski R. Analysis of microplastics in consumer products by single particle-inductively coupled plasma mass spectrometry using the carbon-13 isotope. Talanta 2021;221:121486. https://doi.org/10.1016/J.TALANTA.2020.121486.
- Jiménez-Lamana J, Marigliano L, Allouche J, Grassl B, Szpunar J, Reynaud S. A
 Novel Strategy for the Detection and Quantification of Nanoplastics by Single Particle
 Inductively Coupled Plasma Mass Spectrometry (ICP-MS). Anal Chem
 2020;92:11664–72. https://doi.org/10.1021/acs.analchem.0c01536.
- 1146 [96] Baur S, Reemtsma T, Stärk HJ, Wagner S. Surfactant assisted extraction of incidental nanoparticles from road runoff sediment and their characterization by single particle1148 ICP-MS. Chemosphere 2020;246:125765.
 1149 https://doi.org/10.1016/j.chemosphere.2019.125765.
- Toncelli C, Mylona K, Tsapakis M, Pergantis SA. Flow injection with on-line dilution and single particle inductively coupled plasma-mass spectrometry for monitoring silver nanoparticles in seawater and in marine microorganisms. J Anal At Spectrom 2016;31:1430–9. https://doi.org/10.1039/c6ja00011h.
- 1154 [98] Taboada-López MV, Herbello-Hermelo P, Domínguez-González R, Bermejo-Barrera 1155 P, Moreda-Piñeiro A. Enzymatic hydrolysis as a sample pre-treatment for titanium 1156 dioxide nanoparticles assessment in surimi (crab sticks) by single particle ICP-MS. 1157 Talanta 2019;195:23–32. https://doi.org/10.1016/j.talanta.2018.11.023.
- 1158 [99] Vidmar J, Buerki-Thurnherr T, Loeschner K. Comparison of the suitability of alkaline 1159 or enzymatic sample pre-treatment for characterization of silver nanoparticles in human 1160 tissue by single particle ICP-MS. J Anal At Spectrom 2018;33:752–61. 1161 https://doi.org/10.1039/c7ja00402h.
- 1162 [100] Tharaud M, Louvat P, Benedetti MF. Detection of nanoparticles by single-particle ICP-1163 MS with complete transport efficiency through direct nebulization at few-microlitres-1164 per-minute uptake rates. Anal Bioanal Chem 2021;413:923–33. 1165 https://doi.org/10.1007/s00216-020-03048-y.
- [101] Lin FH, Miyashita SI, Inagaki K, Liu YH, Hsu IH. Evaluation of three different sample
 introduction systems for single-particle inductively coupled plasma mass spectrometry

- 1168 (spICP-MS) applications. J Anal At Spectrom 2019;34:401–6. 1169 https://doi.org/10.1039/c8ja00295a.
- 1170 [102] Miyashita S ichi, Mitsuhashi H, Fujii S ichiro, Takatsu A, Inagaki K, Fujimoto T. High 1171 transport efficiency of nanoparticles through a total-consumption sample introduction 1172 system and its beneficial application for particle size evaluation in single-particle ICP-1173 MS. Anal Bioanal Chem 2017;409:1531–45. https://doi.org/10.1007/s00216-016-0089-1174 5.
- [103] Hadioui M, Knapp G, Azimzada A, Jreije I, Frechette-Viens L, Wilkinson KJ.
 Lowering the Size Detection Limits of Ag and TiO2 Nanoparticles by Single Particle
 ICP-MS. Anal Chem 2019;91:13275–84.
 https://doi.org/10.1021/acs.analchem.9b04007.
- 1179 [104] Cao Y, Feng J, Tang L, Yu C, Mo G, Deng B. A highly efficient introduction system 1180 for single cell- ICP-MS and its application to detection of copper in single human red 1181 blood cells. Talanta 2020;206. https://doi.org/10.1016/j.talanta.2019.120174.
- [105] Gundlach-Graham A, Mehrabi K. Monodisperse microdroplets: A tool that advances single-particle ICP-MS measurements. J Anal At Spectrom 2020;35:1727–39.
 https://doi.org/10.1039/d0ja00213e.
- 1185 [106] Tuoriniemi J, Holbrook TR, Cornelis G, Schmitt M, Stärk HJ, Wagner S. Measurement 1186 of number concentrations and sizes of Au nano-particles spiked into soil by laser 1187 ablation single particle ICPMS. J Anal At Spectrom 2020;35:1678–86. 1188 https://doi.org/10.1039/d0ja00243g.
- 1189 [107] Vidmar J, Loeschner K, Correia M, Larsen EH, Manser P, Wichser A, et al.
 1190 Translocation of silver nanoparticles in the: Ex vivo human placenta perfusion model
 1191 characterized by single particle ICP-MS. Nanoscale 2018;10:11980–91.
 1192 https://doi.org/10.1039/c8nr02096e.
- [108] Candás-Zapico S, Kutscher DJ, Montes-Bayón M, Bettmer J. Single particle analysis
 of TiO2 in candy products using triple quadrupole ICP-MS. Talanta 2018;180:309–15.
 https://doi.org/10.1016/j.talanta.2017.12.041.
- [109] Venkatesan AK, Rodríguez BT, Marcotte AR, Bi X, Schoepf J, Ranville JF, et al.
 Using single-particle ICP-MS for monitoring metal-containing particles in tap water.
 Environ Sci Water Res Technol 2018;4:1923–32. https://doi.org/10.1039/c8ew00478a.
- [110] Gondikas A, Von Der Kammer F, Kaegi R, Borovinskaya O, Neubauer E, Navratilova J, et al. Where is the nano? Analytical approaches for the detection and quantification of TiO2 engineered nanoparticles in surface waters. Environ Sci Nano 2018;5:313–26. https://doi.org/10.1039/c7en00952f.
- [111] Kaegi R, Englert A, Gondikas A, Sinnet B, von der Kammer F, Burkhardt M. Release
 of TiO2 (Nano) particles from construction and demolition landfills. NanoImpact
 2017;8:73–9. https://doi.org/10.1016/j.impact.2017.07.004.
- 1206 [112] Navratilova J, Praetorius A, Gondikas A, Fabienke W, von der Kammer F, Hofmann T.
 1207 Detection of engineered copper nanoparticles in soil using single particle ICP-MS. Int J
 1208 Environ Res Public Health 2015;12:15756–68.
- [113] Wojcieszek J, Jiménez-Lamana J, Bierla K, Asztemborska M, Ruzik L, Jarosz M, et al.
 Elucidation of the fate of zinc in model plants using single particle ICP-MS and ESI
 tandem MS. J Anal At Spectrom 2019;34:683–93. https://doi.org/10.1039/c8ja00390d.
- 1212 [114] Hassellöv M, Lyvén B, Haraldsson C, Sirinawin W. Determination of continuous size 1213 and trace element distribution of colloidal material in natural water by on-line coupling 1214 of flow field-flow fractionation with ICPMS. Anal Chem 1999;71:3497–502. 1215 https://doi.org/10.1021/ac981455y.
- [115] Hassellv M, Kaegi R. Analysis and Characterization of Manufactured Nanoparticles in
 Aquatic Environments. Environ. Hum. Heal. Impacts Nanotechnol., Chichester, UK:

- 1218 John Wiley & Sons, Ltd; 2009, p. 211–66. 1219 https://doi.org/10.1002/9781444307504.ch6.
- 1220 [116] Hennebert P, Avellan A, Yan J, Aguerre-Chariol O. Experimental evidence of colloids 1221 and nanoparticles presence from 25 waste leachates. Waste Manag 2013;33:1870–81. 1222 https://doi.org/10.1016/j.wasman.2013.04.014.
- 1223 [117] Tiede K, Boxall A, Tear S, Lewis J, David H, Hassellov M. Detection and characterization of engineered nanoparticles in food and the environment. Food Addit 1225 Contam Part A 2008;25:795–821. https://doi.org/10.1080/02652030802007553.
- 1226 [118] Ilett M, Matar O, Bamiduro F, Sanchez-Segado S, Brydson R, Brown A, et al.
 1227 Nanoparticle corona artefacts derived from specimen preparation of particle suspensions. Sci Rep 2020;10:1–6. https://doi.org/10.1038/s41598-020-62253-y.
- [119] Michen B, Geers C, Vanhecke D, Endes C, Rothen-Rutishauser B, Balog S, et al.
 Avoiding drying-artifacts in transmission electron microscopy: Characterizing the size and colloidal state of nanoparticles. Sci Rep 2015;5:9793.
 https://doi.org/10.1038/srep09793.
- [120] Urstoeger A, Wimmer A, Kaegi R, Reiter S, Schuster M. Looking at Silver-Based
 Nanoparticles in Environmental Water Samples: Repetitive Cloud Point Extraction
 Bridges Gaps in Electron Microscopy for Naturally Occurring Nanoparticles. Environ
 Sci Technol 2020;54:12063-71. https://doi.org/10.1021/ACS.EST.0C02878.
- [121] Griffin BJ. Variable Pressure and Environmental Scanning Electron Microscopy. From
 Methods Mol. Biol., vol. 369, Humana Press; 2007, p. 467–95.
 https://doi.org/10.1007/978-1-59745-294-6 23.
- 1240 [122] Cooper DA, Corcoran PL. Effects of mechanical and chemical processes on the 1241 degradation of plastic beach debris on the island of Kauai, Hawaii. Mar Pollut Bull 1242 2010;60:650–4. https://doi.org/10.1016/j.marpolbul.2009.12.026.
- [123] Zuccarello P, Ferrante M, Cristaldi A, Copat C, Grasso A, Sangregorio D, et al.
 Exposure to microplastics (<10 μm) associated to plastic bottles mineral water
 consumption: The first quantitative study. Water Res 2019;157:365–71.
 https://doi.org/10.1016/j.watres.2019.03.091.
- 1247 [124] Oßmann B, Schymanski D, Ivleva NP, Fischer D, Fischer F, Dallmann G, et al.
 1248 Comment on "exposure to microplastics (<10 Mm) associated to plastic bottles mineral
 1249 water consumption: The first quantitative study by Zuccarello et al. [Water Research
 1250 157 (2019) 365–371]." Water Res 2019;162:516–7.
 1251 https://doi.org/10.1016/j.watres.2019.06.032.
- 1252 [125] Pivokonsky M, Cermakova L, Novotna K, Peer P, Cajthaml T, Janda V. Occurrence of microplastics in raw and treated drinking water. Sci Total Environ 2018;643:1644–51. https://doi.org/10.1016/j.scitotenv.2018.08.102.
- 1255 [126] Filipe V, Hawe A, Jiskoot W. Critical evaluation of nanoparticle tracking analysis
 1256 (NTA) by NanoSight for the measurement of nanoparticles and protein aggregates.
 1257 Pharm Res 2010;27:796–810. https://doi.org/10.1007/s11095-010-0073-2.
- 1258 [127] Pecora R. Quasi-elastic light scattering from macromolecules. Annu Rev Biophys Bioeng 1972;1:257–76. https://doi.org/10.1146/annurev.bb.01.060172.001353.
- 1260 [128] Silbey R, Deutch JM. Quasielastic light scattering from large macromolecules. J Chem Phys 1972;57:5010–1. https://doi.org/10.1063/1.1678173.
- [129] McElfresh C, Harrington T, Vecchio KS. Application of a novel new multispectral
 nanoparticle tracking technique. Meas Sci Technol 2018;29:065002.
 https://doi.org/10.1088/1361-6501/aab940.
- 1265 [130] Hackley VA. Measuring the Size of Nanoparticles in Aqueous Media Using Batch-1266 Mode Dynamic Light Scattering 2015. https://doi.org/10.6028/NIST.SP.1200-6.
- 1267 [131] Provencher SW. CONTIN: A general purpose constrained regularization program for

- inverting noisy linear algebraic and integral equations. Comput Phys Commun 1982;27:229–42. https://doi.org/10.1016/0010-4655(82)90174-6.
- [132] Scotti A, Liu W, Hyatt JS, Herman ES, Choi HS, Kim JW, et al. The CONTIN
 algorithm and its application to determine the size distribution of microgel suspensions.
 J Chem Phys 2015;142:234905. https://doi.org/10.1063/1.4921686.
- 1273 [133] Silmore KS, Gong X, Strano MS, Swan JW. High-resolution nanoparticle sizing with maximum a posteriori nanoparticle tracking analysis. ACS Nano 2019;13:3940–52. https://doi.org/10.1021/acsnano.8b07215.
- 1276 [134] Malm A V., Corbett JCW. Improved Dynamic Light Scattering using an adaptive and statistically driven time resolved treatment of correlation data. Sci Rep 2019;9:1–11. https://doi.org/10.1038/s41598-019-50077-4.
- [135] Schintke S, Frau E. Modulated 3D Cross-Correlation Dynamic Light Scattering
 Applications for Optical Biosensing and Time-Dependent Monitoring of Nanoparticle Biofluid Interactions. Appl Sci 2020;10:8969. https://doi.org/10.3390/app10248969.
- [136] Block ID, Scheffold F. Modulated 3D cross-correlation light scattering: Improving turbid sample characterization. Rev Sci Instrum 2010;81:123107.
 https://doi.org/10.1063/1.3518961.
- [137] Dhadwal HS, Ansari RR, Meyer W V. A fiber-optic probe for particle sizing in concentrated suspensions. Rev Sci Instrum 1991;62:2963–8.
 https://doi.org/10.1063/1.1142190.
- 1288 [138] Dhadwal HS, Khan RR, Suh K. Integrated fiber optic probe for dynamic light scattering. Appl Opt 1993;32:3901. https://doi.org/10.1364/ao.32.003901.
- 1290 [139] Challis RE, Povey MJW, Mather ML, Holmes AK. Ultrasound techniques for characterizing colloidal dispersions. Reports Prog Phys 2005;68:1541–637. https://doi.org/10.1088/0034-4885/68/7/R01.
- 1293 [140] McClements DJ, Coupland JN. Theory of droplet size distribution measurements in 1294 emulsions using ultrasonic spectroscopy. Colloids Surfaces A Physicochem Eng Asp 1295 1996;117:161–70. https://doi.org/10.1016/0927-7757(96)03673-4.
- 1296 [141] Zhou W, Su M, Cai X. Advances in nanoparticle sizing in suspensions: Dynamic light
 1297 scattering and ultrasonic attenuation spectroscopy. KONA Powder Part J
 1298 2017;2017:168–82. https://doi.org/10.14356/kona.2017022.
- [142] Mehrabi K, Nowack B, Arroyo Rojas Dasilva Y, Mitrano DM. Improvements in Nanoparticle Tracking Analysis to Measure Particle Aggregation and Mass
 Distribution: A Case Study on Engineered Nanomaterial Stability in Incineration
 Landfill Leachates. Environ Sci Technol 2017;51:5611–21.
 https://doi.org/10.1021/acs.est.7b00597.
- [143] Gondikas A, Gallego-Urrea J, Halbach M, Derrien N, Hassellöv M. Nanomaterial Fate
 in Seawater: A Rapid Sink or Intermittent Stabilization? Front Environ Sci 2020;8:151.
 https://doi.org/10.3389/fenvs.2020.00151.
- 1307 [144] Guerra LF, Muir TW, Yang H. Single-Particle Dynamic Light Scattering: Shapes of
 1308 Individual Nanoparticles. Nano Lett 2019;19:5530–6.
 1309 https://doi.org/10.1021/acs.nanolett.9b02066.
- 1310 [145] Xu C, Cai X, Zhang J, Liu L. Fast nanoparticle sizing by image dynamic light 1311 scattering. Particuology 2015;19:82–5. https://doi.org/10.1016/j.partic.2014.04.014.
- 1312 [146] Schimpf ME. Field-Flow Fractionation Handbook. John Wiley & Sons, Inc.; 2000.
- 1313 [147] Gigault J, El Hadri H, Reynaud S, Deniau E, Grassl B. Asymmetrical flow field flow fractionation methods to characterize submicron particles: application to carbon-based aggregates and nanoplastics. Anal Bioanal Chem 2017;409:6761–9.

 1316 https://doi.org/10.1007/s00216-017-0629-7.
- 1317 [148] Kim YB, Yang JS, Moon MH. Investigation of steric transition with field programming

- in frit inlet asymmetrical flow field-flow fractionation. J Chromatogr A 2018;1576:131–6. https://doi.org/10.1016/j.chroma.2018.09.036.
- [149] Wang Y, Cuss CW, Shotyk W. Application of asymmetric flow field-flow
 fractionation to the study of aquatic systems: Coupled methods, challenges, and future
 needs. J Chromatogr A 2020;1632:461600.
 https://doi.org/10.1016/j.chroma.2020.461600.
- 1324 [150] Correia M, Loeschner K. Detection of nanoplastics in food by asymmetric flow field-1325 flow fractionation coupled to multi-angle light scattering: possibilities, challenges and 1326 analytical limitations. Anal Bioanal Chem 2018;410:5603–15. 1327 https://doi.org/10.1007/s00216-018-0919-8.
- 1328 [151] Mintenig SM, Bäuerlein PS, Koelmans AA, Dekker SC, Van Wezel AP. Closing the gap between small and smaller: towards a framework to analyse nano- and microplastics in aqueous environmental samples. Environ Sci Nano 2018;5:1640–9. https://doi.org/10.1039/c8en00186c.
- 1332 [152] El Hadri H, Gigault J, Tan J, Hackley VA. An assessment of retention behavior for gold nanorods in asymmetrical flow field-flow fractionation. Anal Bioanal Chem 2018;410:6977–84. https://doi.org/10.1007/s00216-018-1325-y.
- [153] Chen M, Parot J, Mukherjee A, Couillard M, Zou S, Hackley VA, et al.
 Characterization of size and aggregation for cellulose nanocrystal dispersions separated
 by asymmetrical-flow field-flow fractionation. Cellulose 2020;27:2015–28.
 https://doi.org/10.1007/s10570-019-02909-9.
- 1339 [154] López-Sanz S, Fariñas NR, Zougagh M, Del Martín-Doimeadios RCR, Ríos Á. AF4-1340 ICP-MS as a powerful tool for the separation of gold nanorods and nanospheres. J Anal 1341 At Spectrom 2020;35:1530–6. https://doi.org/10.1039/d0ja00123f.
- [155] Nguyen T, Liu J, Hackley V. Fractionation and Characterization of High Aspect Ratio
 Gold Nanorods Using Asymmetric-Flow Field Flow Fractionation and Single Particle
 Inductively Coupled Plasma Mass Spectrometry. Chromatography 2015;2:422–35.
 https://doi.org/10.3390/chromatography2030422.
- 1346 [156] Kato H, Nakamura A, Banno H. Determination of number-based size distribution of
 1347 silica particles using centrifugal field-flow fractionation. J Chromatogr A
 1348 2019;1602:409–18. https://doi.org/10.1016/j.chroma.2019.05.055.
- 1349 [157] Niezabitowska E, Town AR, Sabagh B, Morales Moctezuma MD, Kearns VR, Spain SG, et al. Insights into the internal structures of nanogels using a versatile asymmetric-flow field-flow fractionation method. Nanoscale Adv 2020;2:4713–21. https://doi.org/10.1039/d0na00314j.
- [158] Iavicoli P, Urbán P, Bella A, Ryadnov MG, Rossi F, Calzolai L. Application of
 Asymmetric Flow Field-Flow Fractionation hyphenations for liposome-antimicrobial
 peptide interaction. J Chromatogr A 2015;1422:260–9.
 https://doi.org/10.1016/j.chroma.2015.10.029.
- [159] Abdelmohsen LKEA, Rikken RSM, Christianen PCM, van Hest JCM, Wilson DA.
 Shape characterization of polymersome morphologies via light scattering techniques.
 Polymer (Guildf) 2016;107:445–9. https://doi.org/10.1016/j.polymer.2016.06.067.
- [160] Wauters AC, Pijpers IAB, Mason AF, Williams DS, Tel J, Abdelmohsen LKEA, et al.
 Development of Morphologically Discrete PEG-PDLLA Nanotubes for Precision
 Nanomedicine. Biomacromolecules 2019;20:177–83.
 https://doi.org/10.1021/acs.biomac.8b01245.
- 1364 [161] Mukherjee A, Hackley VA. Separation and characterization of cellulose nanocrystals by multi-detector asymmetrical-flow field-flow fractionation. Analyst 2018;143:731–40. https://doi.org/10.1039/c7an01739a.
- 1367 [162] ISO ISO/TS 21362:2018 Nanotechnologies Analysis of nano-objects using

- asymmetrical-flow and centrifugal field-flow fractionation n.d.:38. https://www.iso.org/standard/70761.html (accessed March 23, 2021).
- [163] Sitar S, Vezocňik V, Macěk P, Kogej K, Pahovnik D, Žagar E. Pitfalls in size characterization of soft particles by dynamic light scattering online coupled to asymmetrical flow field-flow fractionation. Anal Chem 2017;89:42.
 https://doi.org/10.1021/acs.analchem.7b03251.
- 1374 [164] Adkins GB, Sun E, Coreas R, Zhong W. Asymmetrical Flow Field Flow Fractionation
 1375 Coupled to Nanoparticle Tracking Analysis for Rapid Online Characterization of
 1376 Nanomaterials. Anal Chem 2020;92:7071-8.
 1377 https://doi.org/10.1021/acs.analchem.0c00406.
- 1378 [165] Nischwitz V, Gottselig N, Braun M. Preparative field flow fractionation for complex environmental samples: online detection by inductively coupled plasma mass spectrometry and offline detection by gas chromatography with flame ionization. J Chromatogr A 2020;1632:461581. https://doi.org/10.1016/j.chroma.2020.461581.
- 1382 [166] Marassi V, Roda B, Casolari S, Ortelli S, Blosi M, Zattoni A, et al. Hollow-fiber flow 1383 field-flow fractionation and multi-angle light scattering as a new analytical solution for 1384 quality control in pharmaceutical nanotechnology. Microchem J 2018;136:149–56. 1385 https://doi.org/10.1016/j.microc.2016.12.015.
- 1386 [167] Nabi MM, Wang J, Meyer M, Croteau MN, Ismail N, Baalousha M. Concentrations 1387 and size distribution of TiO2 and Ag engineered particles in five wastewater treatment 1388 plants in the United States. Sci Total Environ 2021;753:142017. 1389 https://doi.org/10.1016/j.scitotenv.2020.142017.
- 1390 [168] Faucher S, Charron G, Lützen E, Le Coustumer P, Schaumlöffel D, Sivry Y, et al.
 1391 Characterization of polymer-coated CdSe/ZnS quantum dots and investigation of their
 1392 behaviour in soil solution at relevant concentration by asymmetric flow field-flow
 1393 fractionation multi angle light scattering inductively coupled plasma mass
 1394 spectrometry. Anal Chim Acta 2018;1028:104–12.
 1395 https://doi.org/10.1016/j.aca.2018.03.051.
- [169] El Hadri H, Louie SM, Hackley VA. Assessing the interactions of metal nanoparticles in soil and sediment matrices-a quantitative analytical multi-technique approach.
 Environ Sci Nano 2018;5:203–14. https://doi.org/10.1039/c7en00868f.
- [170] Mitrano DM, Beltzung A, Frehland S, Schmiedgruber M, Cingolani A, Schmidt F.
 Synthesis of metal-doped nanoplastics and their utility to investigate fate and behaviour in complex environmental systems. Nat Nanotechnol 2019;14:362–8.
 https://doi.org/10.1038/s41565-018-0360-3.
- [171] Barber A, Kly S, Moffitt MG, Rand L, Ranville JF. Coupling single particle ICP-MS
 with field-flow fractionation for characterizing metal nanoparticles contained in
 nanoplastic colloids. Environ Sci Nano 2020;7:514–24.
 https://doi.org/10.1039/c9en00637k.
- Löwa N, Meier F, Welz R, Kratz H, Paysen H, Schnorr J, et al. Novel platform for the multidimensional analysis of magnetic nanoparticles. J Magn Magn Mater
 2021;518:167443. https://doi.org/10.1016/j.jmmm.2020.167443.
- 1410 [173] Herrero P, Bäuerlein PS, Emke E, Pocurull E, de Voogt P. Asymmetrical flow field-1411 flow fractionation hyphenated to Orbitrap high resolution mass spectrometry for the 1412 determination of (functionalised) aqueous fullerene aggregates. J Chromatogr A 1413 2014;1356:277–82. https://doi.org/10.1016/j.chroma.2014.06.068.
- 1414 [174] Gigault J, Pettibone JM, Schmitt C, Hackley VA. Rational strategy for characterization 1415 of nanoscale particles by asymmetric-flow field flow fractionation: A tutorial. Anal 1416 Chim Acta 2014;809:9–24. https://doi.org/10.1016/j.aca.2013.11.021.
- 1417 [175] GESAMP. Guidelines for the Monitoring and Assessment of Plastic Litter in the Ocean

1418	. 2019.
1419	[176] Mattsson K, Björkroth F, Karlsson T, Hassellöv M. Nanofragmentation of Expanded
1420	Polystyrene Under Simulated Environmental Weathering (Thermooxidative
1421	Degradation and Hydrodynamic Turbulence). Front Mar Sci 2021;7:1252.
1422	https://doi.org/10.3389/fmars.2020.578178.
1423	